Czech University of Life Sciences Prague
Faculty of Environmental Sciences

Modelling Hydrological Balance Using Lumped and Semi-distributed Hydrological Model

MASTER THESIS of

Hatice TURK

A thesis submitted in partial fulfillment for the
Master Degree

in the

Department of Water Resources and Environmental Modelling
Faculty of Environmental Sciences
Czech University of Life Sciences Prague

Supervisor:
doc. Ing Petr Máca, Ph.D.
25.03.2021

CZECH UNIVERSITY OF LIFE SCIENCES PRAGUE

Faculty of Environmental Sciences

DIPLOMA THESIS ASSIGNMENT

B.Sc. Hatice Türk

Landscape Engineering
Environmental Modelling

Thesis title

Modelling hydrological balance using lumped and semi-distributed hydrological model

---

Objectives of thesis

The thesis aims to implement dHRUM model on the selected river basins. Both lumped and semi-distributed versions of dHRUM model will be prepared and tested on a chosen set of catchments.

Methodology

The methodology is composed of the following main steps:

1. Select and prepare the data for hydrological balance modelling at the chosen catchment
2. Implement the dHRUM model on selected watershed
3. Calibrate dHRUM models
4. Validate dHRUM models

Author Acknowledgments

I would like to thank doc. Ing Petr Máca, Ph.D. for his advice and support during my work on this thesis.

Hatice Turk

I declare that I have worked on my diploma thesis titled **"Modelling Hydrological Balance Using Lumped and Semi-distributed Hydrological Model"** by myself and I have used only the sources mentioned at the end of the thesis. As the author of the diploma thesis, I declare that the thesis does not break any copyrights.

In Prague on31.03.2021

Hatice Turk

Abstract

Successful water resource management necessitates the use of a well-calibrated hydrological model. A hydrological model aims to properly describe hydrological systems in order to assess the impact and risk that is associated with water resource management in a river basin (Beven, 2006). Accordingly, a clear representation of simplification of the real-world system by using mathematical models and assumptions all together with input and forcing data, model parameters, and their initial values is irresistible.Different multi-objective and multi-base flow filter techniques have been evaluated in this study for the calibration of distributed Hydrological Response Unit Model hydrological model applied to the case of the 671 CONUS catchments with three different forcing data(Maurer, nldas and daymet forcing). The calibration process involved the use of four objective functions from goodness of fit measures (minimizingNSE, minimizingKGE, minimizingIOA, minimizing WSSR) and three base flowfilters (Lyne and Hollick, Chapman and Maxwell, and Eckhardt filters).The calibration scenarios applied showed that they were capable of predicting runoff with a reasonable level of accuracy for most cases. For the particular case of Maurer forcing, its found that the objective function of nse and Eckhardt base flow filter methods performed best for both total run of and base flow generations.

Keywords: Hydrological modelling, Multi- objective function calibration, low-flow indices, CAMELS data set

Contents

List of Figures

List of Tables

CHAPTER 1

Introduction

1.1 Objectives of the thesis

The objective of this study is to evaluate the calibration performance of the Distributed hydrological response Unit Model(DHRUM). In other words, this study is an approach to implement multiple calibration scenarios to a hydrological model to demonstrate the model performance improvement. The first focus is to evaluate if it is sufficient to calibrate the dHRUM model only using a single objective function or using a linear combination of multiple objective functions. The second focus is to underline if it is sufficient to calibrate the dHRUM model by using different base flow filters and to underline if there will be any improvement by a linear combination of different objective functions and base flow filters. By the same token, these study focused on analysing impact of different forcing data on model calibration performance.

1.2 Literature review

Successful water resource management necessitates the use of a well-calibrated hydrological model. A hydrological model aims to properly describe hydrological systems in order to assess the impact and risk that is associated with water resource management in a river basin (Beven, 2006). To do so, a clear representation of simplification of the real-world system by using mathematical models and assumptions all together with input and forcing data, model parameters, and their initial values is irresistible.

The conceptual rainfall-runoff models are commonly used to investigate the relationships between the meteorological and hydrological data. The rainfall-runoff model used in this study is distributed Hydrological Response Unit Model(dHRUM) which can be used as a distributed or lumped model. For this research the model used as the lumped model, which means that the model using only single precipitation and air temperature data series to represent the whole catchment. Fine points of the dHRUM model are described in the methodology section.

There are several rainfall-runoff models classified as distributed like ATHYS which is a

conceptual distributed model (Mishra, Singh, 2013) or Conceptual lumped rainfall-runoff models such as HBV model VIC model, HYMOD model are commonly used, for a wide range of environmental problems. (Beven, 2006; Zhang et al., 2008; Yu, Yang, 2000). Every hydrological model consists of a set of a parameter to be optimized. Even if the parameters of theoretical rainfall-runoff models have some physical representation, they also often required effective calibration on measured data to be applied to a particular catchment.

There are numeraous optimization algorithms such as Shuffled Complex Evolution (SCE-UA), Genetic algorithms (GAs), Genetic learning particle swarm optimization(GLPSO) effectively used for parameter calibrations of a model (Duan et al., 1992; Mitsos et al., 2008). Each optimization algorithm has the same goal which is to find the best value for model parameters based on numerical goodness-of-fit measures like minimizing or maximizing an objective function. In this study optimisation algorithm of GlobalOptimisationn by Differential Evolution introduced by Storn, Price (1997) is used for model parameter optimizations. Differential Evolution (DE) belongs to the class of genetic algorithms (GAs) and it is useful for the solution of global optimization problems. (Li et al., 2009; Ardia et al., 2011)

In general, the most popular measure of the fit of the model is single objective functions such as the Nash-Sutcliffe efficiency coefficient (NSE), coefficient of determination (R2) and the relative volume error (RE) of the hydrograph, Kling Gupta Efficiency. (Yu, Yang, 2000; Jie et al., 2016; Kim et al., 2018; Gupta et al., 2009). Every single objective function can be used for different purposes. For example, Gar (2017) find that the Kling and Gupta efficiency (KGE) applied to a transformation of discharge is inadequate to calibrate rainfall-runoff models for low-flow index simulations. On the other hand, Kim et al. (2018)find that the Weighted Sum of Squared of Residual (WSSR) is adequate in peak flow simulation for estimation peak flood runoff. Furthermore, Fowler et al. (2018) has shown that Split KGE which is a Time-based meta-objective function that gives equal weight to each year in the calibration series result in significantly better split-sample results than least-squares approaches for simulations in a drying climate.

Despite the single objective functions has adequate calibration results for special cases and purposes, when all the characteristics of a hydrograph demand to be duplicated in real applications, then it is not feasible for a single objective function to be efficient enough to calibrate the selected model (Jie et al., 2016). There are many studies that showed that the application of multi-objective functions to calibrate the parameters of hydrological models perform better than single ones. (Jie et al., 2016; Yapo et al., 1998; Gupta et al., 2009; Piotrowski et al., 2019; Adeyeri et al., 2020). Furthermore, The better performance of the combination of objective functions is not only verified for rainfall-runoff forecasting but also verified to Derived Optimal Linear Combination Evapotranspiration (Hobeichi et al., 2018).

On the other hand, many studies focused on better model calibration for the component of stream flow which are direct runoff and base flow separately. There are many studies focused on more accurate simulation and estimation of the base flow component of total runoff. For

example, Ferket et al. (2010) has compared two commonly used rainfall-runoff models (HBC, PDM) using base flow estimates to validate internal model dynamics. Moreover Staudinger et al. (2011) study on comparison of hydrological model structures based on recession and low flow simulations and showed that simulations of summer low flows were weaker than simulations of winter low flows. Besides, there are several studies for better estimation of base flow by implementation of base flow filters (Eckhardt, 2008; Chapman, 1999; Lyne, Hollick, 1979)

In short, In this study dHRUM model is used for water balance calculations. Fine points of the dHRUM model are described in the methodology section. The model implemented to 671 the contiguous United States (CONUS) catchments utilizing analyzed time series that are selected from Catchment Attributes and Meteorology for Large-sample Studies(CAMELS). During the calibration processes of the model three main scenarios are followed to analyse model performance variations. The first scenario is the calibration of the dHRUM model parameters by total runoff generationswith a single objective function from four different classes which are Nash- Sutcliffe efficiency, Kling-Gupta Efficiency(KGE), Index of agreement(IOA) and Weighted Sum of Squared of Residual (WSSR). The second scenario is the calibration of the dHRUM model parameters by base flow generation with implementations of single base flow filter function from three different base flow filters which are Lyne and Hollick, Chapman and Maxwell, and Eckhardt digital filters. The last scenario is the calibration of the dHRUM model parameters by a linear combination of objective functions used during scenario one and two. For every scenario model calibration performance are valuated according to model total runoff and base flow generations. For model calibration performance evaluations three commonly used evaluation criteria are adopted for grading the goodness-of-fit of the 671 CONUS catchments simulated flood hydrographs. These goodness-of-fit measures are averaged Nash-Sutcliffe coefficient, Kling-Gupta Efficiency and Root Mean Square Error(RMSE) out of 671 CONUS catchment

CHAPTER 2

Material and Methods

2.1 Material and Methods

The material and methods section is structured as follows. The first section is the the material section and it is describe the study area in detail. Then the methods section describes the hydrological model which is distributed Hydrological Response Unit Model that used in this study. The model structure and water balance equations are described in detail. More over the methods section is explaining the calibration process of the distributed Hydrological Response Unit Model. In this section, the selection of objective functions for testing is described with their equations in detail. Following that the selection of base flow filters and their equations are described in detail. From there on, the optimization algorithm used during model optimization is described briefly. Lastly, the methods section is describing the dHRUM model calibration performance evaluation criteria clearly.

2.1.1 Material

In this study analysed time series are selected from Catchment Attributes and Meteorology for Large-sample Studies(CAMELS). CAMELS data set is a set of attributes for 671 catchments in the contiguous United States (CONUS) with different catchment attributes classes such as climate, topography, vegetation, soil and geology. Those catchments are minimally impacted by human activities. (Newman et al., 2015) In addtion, those catchments cover a broad diverse range of features, from climatic conditions, elevations ranging from 10 to almost 3,600 meters above sea level, and catchment areas ranging from 5 to nearly 26,000 km2. For each catchment, a variety of factors that affect catchment behaviour and hydrological processes are characterised by Addor et al. (2017).

Addor et al. (2017) revised the data set with developed attributes information and their interrelationships. They retrieved topographic characteristics of catchments from Newman et al. (2015) study on the Development of a large-sample watershed-scale hydrometeorological data set for the contiguous USA. Additionally, Addor et al. (2017)prepare data of climatic indices such us

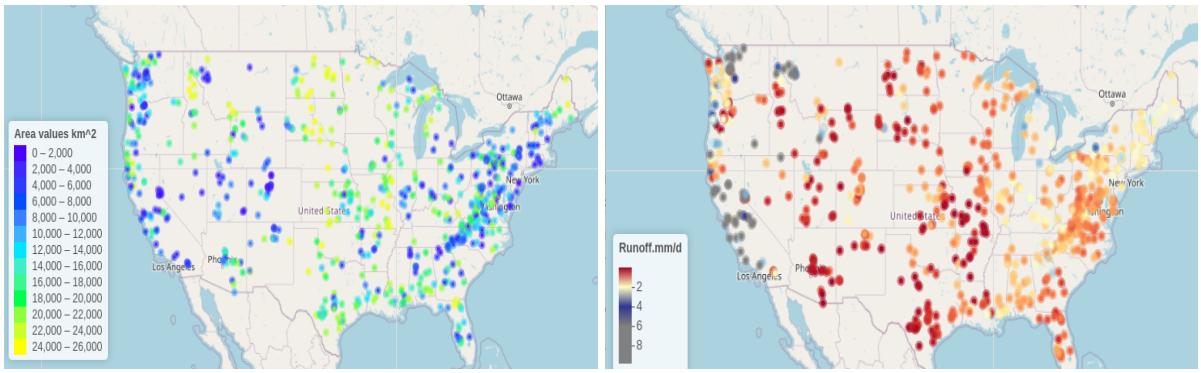

Figure 2.1: CAMEL data set with 671 Catchments Area and Stream flow distribution maps

aridity and dry day frequencies, hydrological signatures like base flow index, by computing time series data of catchments which provided by Newman et al. (2015). Likewise, soil characteristics, vegetation characteristics and geological characteristics of all 671 catchments were computed by Addor et al. (2017) by drawing back data from State Soil Geographic Database(STATSGO), Moderate Resolution Imaging Spectroradiometer (MODIS), Global Lithological Map(GLiM), GLobal HYdrogeology MaPS(GLHYMPS) data sets. All the catchment attributes introduced provided by Addor et al. (2017) are freely available online. The figure 2.1 show the map of the catchments with Area and annual mean daily stream flow information. Figure left side displays the location of each basin with the area coloured while the figure on the right site is to describe annual mean stream flow as mm/d

Besides the catchment attributes, Camel data set contains all the basin forcing data for three meteorology products which are Daily Surface Weather Data on a 1-km Grid for North America (Daymet), North American Land Data Assimilation System (NLDAS) and Long-Term Hydrologically Based Data set of Land Surface Fluxes and States for the Conterminous United States(Maurer). Those three forcing data sets cover daily continuous data of minimum and maximum temperature, precipitation amount, humidity, shortwave radiation, snow water equivalent, and lastly day length. (Addor et al., 2017) Daymet data is available from January 1, 1980, to December 31, 2013, with time step at a 1-km x 1-km spatial resolution Thornton et al. (????), while NLDAS forcing data are available from January 1, 1980, to December 31, 2014 and Maurer data is available from January 1, 1980 to December 31, 2008. (Xia et al., 2012; Maurer et al., 2002). Streamflow data from the The United States Geological Survey (USGS) is also available for all basins for all dates available between January 1 and December 31, 2014.

Despite the fact that all three forcing data covers many catchments attributes classes, for this study, precipitation, minimum and maximum temperature, observed streamflow data are mainly used for model calibration. Randomly selected continuous data for precipitation, temperature, and streamflow data corresponding to five years are analysed during the calibration process of dHRUM. The random selection of 5-year data is appropriated from data corresponding fifteen years from 1980 to 1995. Precipitation data is used precisely, however, the temperature data

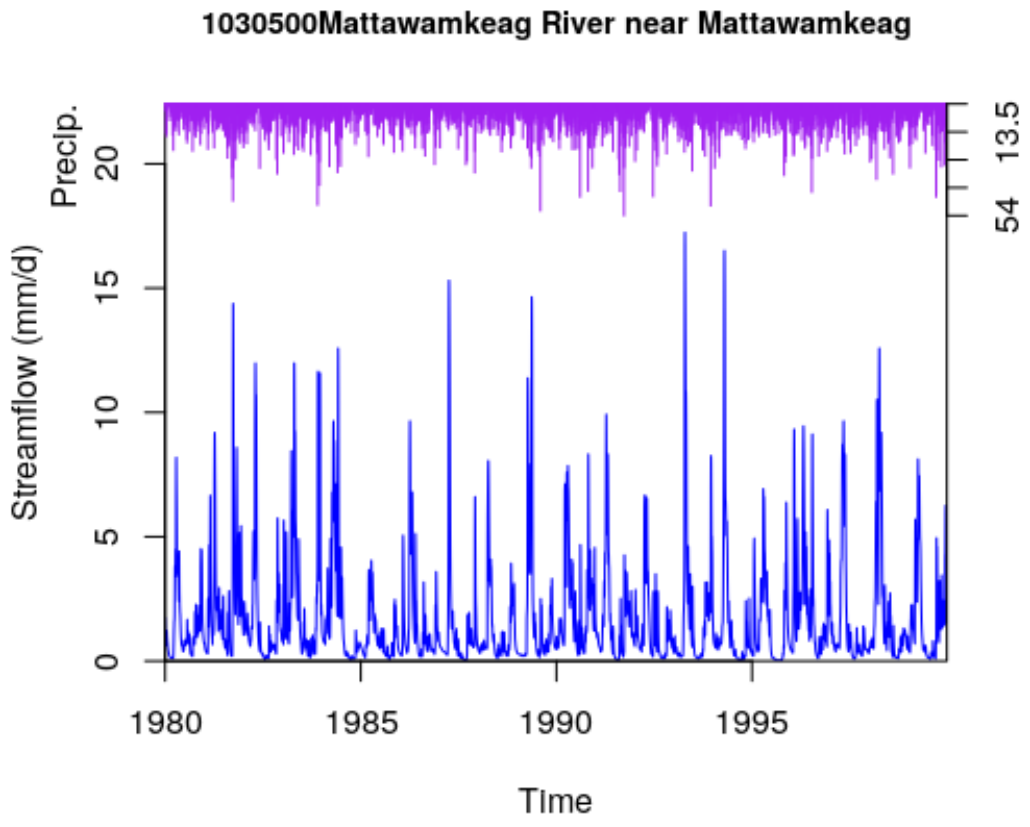

Figure 2.2: Mattawamkeag River near Mattawamkeag streamflow(mm/d) and presipitation(mm/d) time series

is calculated as the mean value of the minimum and maximum temperature data and observed streamflow data is used directly after proper unit conversion of cubic feet per second to milimiter per day as an input data to the model. The figure 2.2 is a representation of precipitation and observed streamflow time series data after proper unit conversions for a catchment with Id of 1030500 and named Mattawamkeag River near Mattawamkeag as an example of data set.

2.1.2 Methods

Description of hydrological model

Distributed Hydrological Response Unit Model(DHRUM) consist of 6 main storage. These are soil storage, groundwater storage, canopy storage, stem storage, snow storage and surface retention storage. Canopy storage, steam storage and snow storage are interception storage. The model work with two main inputs which are precipitation and temperature. The outputs from precipitation and the temperature data consist of 22 consequent components of water balance equations of each storage. These outputs are listed in the table 2.1with their representations and definitions. Despite the model designed for distributed unit calculation in this study the lumped

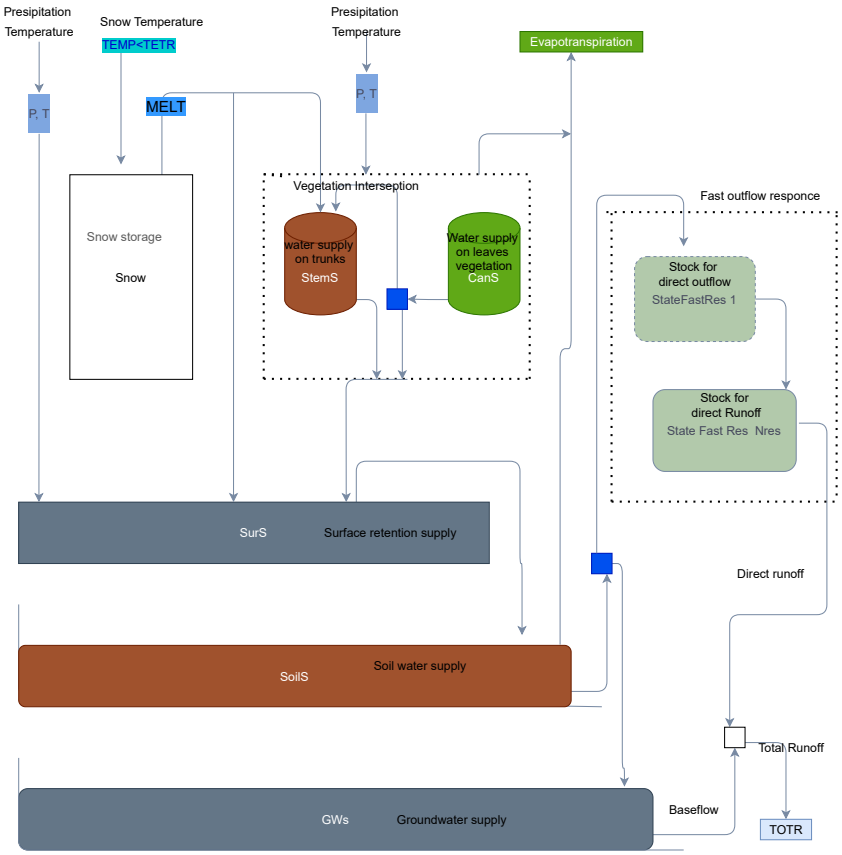

Figure 2.3: Main layout of the DHRUM Model

version of the model taken into consideration. Moreover, the model has 15 parameters inputs for calibration. Those parameters and their definitions are explained in the following sections in detail.

For the further description of the model following steps are explained in the correct order. First of all, the model structure is represented. Fallowing that the model parameter inputs are listed in a table. Secondly, water balance equations of each component of the model are described in brief.

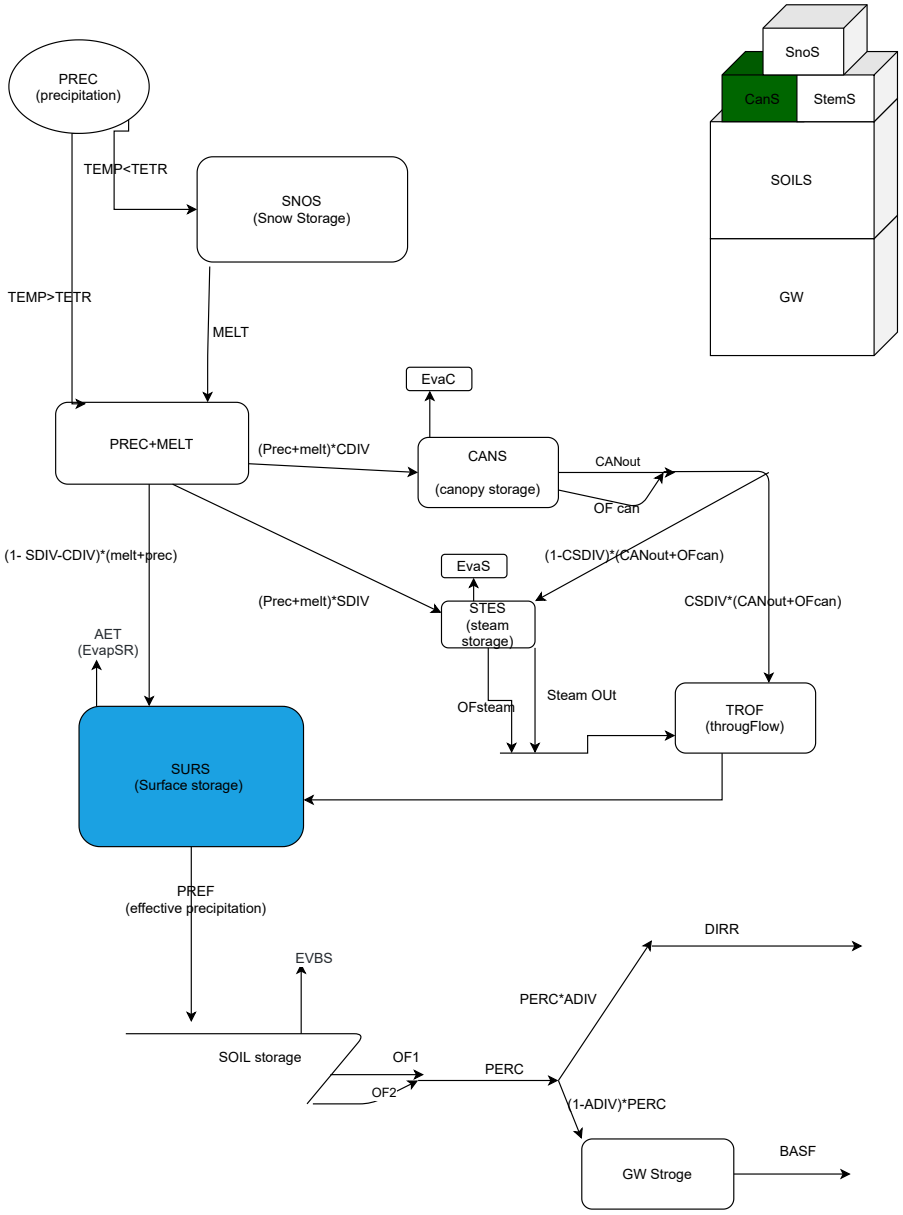

Figure 2.4: Detailed Schematic of the DHRUM Model

Table 2.1: Summary table of dHRUM output generations

	OUTPUT	DEFINITION
1	Prec	Precipitation
2	Snow	Snow depth
3	AEt	Actual Evapotranspiration
4	PEt	Potential Evapotranspiration
5	Temp	Temperature
6	TroF	Through fall
7	SteF	Stem flow
8	CanF	Canopy drainage
9	CanS	Canopy storage
10	SteS	Stem-storage
11	EvaC	Canopy Evaporation
12	EvaS	Stem-evaporation
13	EvbS	Bare soil Evapotranspiration
14	IntS	Interception storage
15	SoiS	Soil storage
16	GroS	Groundwater storage
17	SurS	Surface retention
18	TotR	Total-runoff
19	Basf	Base-flow
20	DirR	Direct Runoff
21	Melt	Melting
22	Perc	Percolation

The rainfall–runoff model DHRUM Model structure and calibration parameters

The figure 2.4 is a clear representation of the structure of the distributed Hydrological Response Unit Model. The parameters named in the figure are listed in the following table with their definitions. As it is mentioned before, dHRUM consists of 3 interception storage which is, snow, canopy and stem storage and three linear reservoirs of bare soil storage, groundwater storage. In addition, The DHRUM model calculates 4 part of evaporation which evaporation from the canopy (EVAC, mm), evaporation from the stem(EVAS, mm), evaporation from bare soil(EVBS, mm) and evaporation from surface storage. Total evaporation and evapotranspiration over a grid cell are computed as the sum of all evaporation. The formulation of the total evaporation and potential evapotranspiration methods which are Hamon and Oudin methods are described in the next sections.

dHRUM dynamics of components

The water balance in the dHRUM model follows the continuity equation for each time-step:

$$\Delta S = P + P_m - E - R$$

where ΔS, P, P_m, E, and R are the change of water storage, precipitation, snow melt, evaporation, and runoff, respectively. Within the time step, all units of above variables are mm.

Table 2.2: Summary table of dHRUM input parameters and their definitions

	PARAMETER	DEFINITION
1	BSOIL	Parameter controlling shape of Pareto distribution of soil storage s [0,inf]
2	CMAX	Max storage of storage's distributed by Pareto distribution [0,inf]
3	BEVAP	Parameter controlling soil evapotranspiration [0,infty] how ever [0.5,3]
4	SMAX	Max soil storage calculate using Cmax and bsoil
5	KS	Storage coefficient of groundwater storage [0,1]
6	KF	Storage coefficient of runoff response reservoirs [0,1]
7	ADIV	Divider of percolation into the direct runoff and groundwater input
8	CDIV	Divider of gross rainfall as a Canopy input [0,1]
9	SDIV	Divider of gross rainfall as a Trunk input [0,1]
10	CANST	The Max canopy storage [0,inf]
11	STEMST	The Max stem and trunk storage
12	CSDIV	he divider of canopy outflow to throughflow and stemflow storage [0,1]
13	TETR	The threshold temperature for determining snow [-inf,inf] better [-5,5]
14	DDFA	The day degree model for snow melt [o, inf] better [0,2]
15	TMEL	The threshold temperature for determining melting process [-inf, inf] better [-5,5]
16	RETCAP	The maximum capacity of surface retention [0, inf]

Potential Evapotranspiration

In the dHRUM there are two methods for potential evapotranspiration calculation. Those are Hamon potential evapotranspiration and Oudin potential evapotranspiration. Detail information of both method are as follow:

Hamon Potential Evapotranspiration

$$PET = k(0.165)(216.7)N\frac{e_s}{T + 273.3}$$

PET is potential evapotranspiration [mm day-1]

k is proportionalitycoefficient = 11 [unitless]

N is daytime length [x/12 hours]

es is saturation vapor pressure [mb]

T average monthly temperature [$^{\circ}C$]

es saturation vapor pressure

$$e_s = 6.108e^{\frac{17.27T}{T+273.3}}$$

N - daylight hours in units of 12 hours

$$N = (\frac{24}{\pi})\omega$$

where,

ω is the sunset hour angle [radians]

w - sunset hour angle

$$\omega = \cos^{-1}[-\tan(\delta)\tan(\varphi)]$$

where, φ is latitude [radians]

δ is the declination [radians]

–declination

$$\delta = 0.409 \sin(\frac{2\pi)}{365} J - 1.39)$$

where,
J is the Julian Day of the year.

OUDIN Potential Evapotranspiration

$$PET = \frac{0.408 Ra(T+5)}{100}$$

where

$$Ra = \frac{(24 * 60)}{\pi C dr(\omega \sin(\varphi) \sin(\delta) + \cos(\varphi) \cos(\delta) \sin(\omega)}$$

where r is

$$\delta = 1 + 0.033 \cos(\frac{2\pi}{365} J)$$

Canopy and Stem Storage Dynamics

Canopy storage Dynamics

The water balance equation in the canopy layer (interception) is:

$$\Delta W = c(P + P_m) - E_c - R_c$$

where Wi is canopy intercepted water (mm),
Ec is evaporation from canopy layer (mm),
Rc is sum of (overflow from canopy and canopy out)
C is divider of gross rainfall as a Canopy input.

When there is intercepted water on the canopy, the canopy evaporates at the maximum value. The maximum canopy evaporation (Ec , mm) from each vegetation tile is calculated using the following formulation:

$$E_c = (\frac{W_i}{W_{im}})^{(2/3)}$$

Where W_{im} = CAN_ST The Max canopy storage [0,inf] (mm);
the power of 2/3 is as described by Deardorff (1978).
The overflow from canopy is calculate as:

$$OF_{can} = CANS[i] - CAN_{ST}$$

where
CANS is canopy storage and CANST is the max canopy storage and

$$CanOut = (\frac{W_i}{W_{im}}) * E_c$$

and total flow from canopy is Rc = CanOut+ Overflow_can

STEM Storage Dynamics

$$\Delta W = s(P + P_m) + (1 - c) * R_c - E_s - R_s$$

where Wi is stem intercepted water (mm),
E_s is evaporation from stem layer (mm),
R_c is sum of (overflow from stem and stem runoff) and (mm),
C is divider of gross rainfall as a Canopy input,
s is divider of gross rainfall as a trunk input.
Canopy storage and stem stooge are linear reservoirs. The maximum stem evaporation (Es, mm) from each vegetation tile is calculated using the following formulation:

$$E_s = (\frac{W_i}{W_{im}})^{(2/3)}$$

Where W_{im} = STEM_ST the Max stem and trunk storage (mm);
the power of 2/3 is as described by Deardorff (1978).

$$SteamOut = (\frac{W_i}{W_{im}}) * E_s$$

$$OF_{stem} = StemS[i] - STEM_{ST}$$

where StemS is stem storage and STEMST is the max stem storage. Then total flow from stem is Rs = SteamOut+ Overflow Stem. Now total througflow from canopy and stem reservoirs.

$$TROF = cR_c + R_s$$

Surface retention storage dynamics

Water balance Equation for surface storage is:

$$\Delta S = (1 - c - s)(P + P_m) + TROF - E_s - R$$

where ΔS, P, P_m, E_s, and , R are the change of surface storage, precipitation, snow melt, evaporation from surface, and surface retention and effective precipitation, respectively. Within the time step, all units of above variables are mm. Evaporation from

$$AET = (\frac{W_i}{RETCAP}) * PET$$

Where Wi surface storage, RETCAP is the maximum capacity of surface retention [0, inf], PET is potential evapotranspritaion calculated from (Hamon or Oudin methods)

Soil storage dynamics

Water balance equation for soil storage

$$\Delta S = P - E_s - R$$

where P is effective precipitation calculated from surface storage, Es is evaporation from bare soil and R is total overflow from soil reservoir also called peculation.

$$C = C_{max} * (1 - (1 - \frac{S1(t)}{S_{max}})^{\frac{1}{b+1}})$$

$$S_{max} = \frac{C_{max}}{b+1}$$

where Cmax is the maximum storage capacity of the catchment
b is a dimensionless parameter
Bevap is Parameter controlling soil evapotranspiration. Then overflow from soil storage can be calculated as:

$$OF1 = (C + PREF - C_{max})$$

Where C is critical storage capacity,
PREF is effective presentation calculated from surface reservoir,
Cmax is the maximum storage capacity of the catchment.
Then the infiltration is calculated as:

$$Inf = PREF - OF1$$

now proposed soil water depth is summation of infiltration and an critical storage capacity (C).

Soil buffer which not effect by evapotranspiration is:

$$SOIS = S_{max} * (1 - (1 - \frac{C}{C_{max}})^{(B_{soil}+1)})$$

where BSOIL Parameter controlling shape of Pareto distribution of soil storage, C is soil water depth, Cmax is the maximum storage capacity, Smax is max of water in soil storage calculated by using Cmax and bsoil. Then Overflow can be calculated as:

$$OF2 = Infiltration - SOIS + SOIS(0)$$

Evaporation from bare soil is calculated as:

$$E_{bs} = (1 - (\frac{Smax - SOIS}{Smax})^{B_{evap}}) * PET$$

where Smax is max of water in soil storage calculated by using Cmax and bsoil. Following this distribution the critical storage capacity C*(t) can be calculated as:

Total overflow which is also called perculation is

$$PERC = OF1 + OF2$$

Groundwater storage dynamics

$$\Delta S = (1 - a)P - R$$

whereΔS is change in groundwater storage,
P is peculation from soil reservoir,
R runoff as base flow, a is divider of percolation into the direct runoff and groundwater input.

Snow Storage dynamics

$$\Delta S = P - R$$

where ΔS is change in snow storage, P is precipitation as snow, R is snow melt which is calculated as:

$$MELT = DDFA * (TEMP - TMEL)$$

where DDFA is the day degree model for snow melt, TEMP is temperature at time t, TMEL is the threshold temperature for determining melting process.

2.1.3 Model Calibration

In this section, the calibration processes of the model are defined.Firstly, the selection of the objective function is explained briefly and the equation of each function are described. Secondly, base flow filter selection and their application in the dHRUM model are clarified. thirdly, the optimization algorithm used in this study and the flow chart of model calibration steps is explained. Lastly, the dHRUM calibration evaluation methodologies are described.

Objective functions Selection

Different objective functions determine the goodness of fit of a parameter set in different ways, so one parameter set can provide a good fit for one objective function but a bad fit for another, or vice versa. Though, the proper objective function for goodness of fit model calibration must be determined in order to achieve a more accurate estimate the optimal values of parameters. (Kim et al., 2018). According to the literature review in the previous section, there are several classes of objective function that are expected to provide improved model calibration. Those class can be defined as:
1) bias penalty which increases sensitivity to model bias such as NSE- bias
2) Before least square equations, application of transforms to runoff values. For example,(Gar, 2017) has tested KGE calculated on root-squared transformed discharges to answer Which objective function to calibrate rainfall-runoff models for low-flow index simulations (Gar, 2017)
3)absolute-error approaches intending to minimize the sum of absolute errors such as Index of agreement (Willmott et al., 2012);
4)Meta-objective functions that evaluate various aspects of the flow regime before combining them into a single objective function. In this class, several different measures are estimated, each focusing on different aspects of the flow regime. After that, they're merged into a metafunction. (Zhang et al., 2008)
5) time-based meta-objective functions which is a combination of multiple measures that focused on different sub-periods of the calibration periods and calculated separately. After that, they're merged into a metafunction. For example, split KGE which is the average of the yearly values of KGE that calculated separately for each year in the calibration period.

In this study, four objective functions are selected for calibration of the model from previous studies. These are Nash- Sutcliffe efficiency, Kling-Gupta Efficiency(KGE), Index of agreement(IOA) and Weighted Sum of Squared of Residual (WSSR).

Nash- Sutcliffe efficiency(NSE)

The Nash-Sutcliffe efficiency (NSE) is a normalized statistic that calculates the magnitude of residual variance versus measured data variance. (Nash, Sutcliffe, 1970) Also an indicator to show how well observed versus simulated data fits. While NSE = 1, corresponds to a model that is perfectly matched to the observed data, NSE = 0, correspond that the model's predictions are as accurate as the observed data's mean values. For model calibration minimization of NSE to 0 is used as main fitness function for calibration which is formulated below.

$$NSE = 1 - \frac{\sum_{n=1}^{M}(obs - sim)^2}{\sum_{n=1}^{M}(obs - mean(obs))^2}$$

Where M is number of observation,
obs is observed values
sim is simulated values.

Kling-Gupta Efficiency (KGE)

The Kling-Gupta efficiency (KGE) is an objective function developed by Gupta et al. (2009) KGE is a function of a combination of three components of Nash-Sutcliffe efficiency (NSE) of model errors. Those are correlation, bias, the ratio of variances) In recent years, KGE has become increasingly popular for calibrating and evaluating hydrological models.

$$KGE = 1 - ED_s$$

$$ED_s = \sqrt{(s_1(r-1))^2 + (s_2(vr-1))^2 + (s_3(\beta-1))^2)}$$

where EDs is the Euclidean distance from the ideal point in the scaled space

$$\beta = u_s/u_o$$

$$\alpha = \sigma_s/\sigma_o$$

1) r is the Pearson product-moment correlation coefficient. Ideal value is suggested as 1
2) Beta is the ratio between the mean of the simulated values and the mean of the observed ones. Ideal value is suggested as 1
3) vr is variability ratio, which could be computed using the standard deviation (Alpha) or the coefficient of variation (Gamma) of sim and obs, depending on the value of method 3.1) Alpha is the ratio between the standard deviation of the simulated values and the standard deviation of the observed ones. Ideal value is Alpha=1. 3.2) Gamma is the ratio between the coefficient of variation (CV) of the simulated values to the coefficient of variation of the observed ones. Ideal value is Gamma=1.

Index of Agreement (IOA)

The Index of Agreement (d) developed by Willmott et al. (2012). It is defined as a standardized measure of the degree of model prediction error and varies between 0 and 1. while a value of 1 indicates a perfect match, a value of 0 indicates no agreement (Willmott et al., 2012).

$$d = 1 - [\frac{\sum_{n=1}^{M}((obs - sim)^2}{\sum_{n=1}^{M}((abs(sim - mean(obs)) + abs(obs - mean(obs)))^2)}]$$

Where M is number of observation,
obs is observed values
sim is simulated values.

Weighted Sum of Squared of Residual (WSSR)

Weighted Sum of Squared of Residual (WSSR) is objective function developed by Kim et al. (2018) for peak flood runoff calibration. The function is given by formula below.

$$F = [\sum_{n=1}^{n}(Q_{obs}(i) - Qsim(i))^2]W_1W_2$$

$$W_1 = 1 + \frac{|Q_{obs,peak} - Q_{sim,peak}|}{Q_{obs,peak}}$$

$$W_2 = 1 + \frac{|T_{obs,peak} - T_{sim,peak}|}{T_{obs,peak}}$$

where: i = the number of the observation
Qobs = the observed runoff
Qsim = the simulated runoff,
Qobs,peak = the observed peak flow,
Qsim,peak = the simulated peak flow, Tobs,peak = the time of occurrence of observed peak flow, Tsim,peak = the time of occurrence of simulated peak flow.
W1 in formula represents the relative error of peak flow runoff and it is suggested that it can be used as a weighting value for preventing overestimation and underestimation of peak flow runoff. (Kim et al., 2018)W2 in formula represent the relative error of peak time. It is also suggested that can be used as a weighting value for decreasing lag time error.(Kim et al., 2018)

Base flow filters selection

There are several digital base flow filter equations developed from 1979 to today. The first suggestion the use of digital filters proposed by Lyne, Hollick (1979). The filter is based on one parameter algorithm which is shown in the equations below. Then, Chapman and Maxwell reformulate the filter equation developed by Lyne, Hollick (1979) due to the insufficient respond of base flow calculation when there was no direct runoff. The reformulation was based on the base flow to be the weighted average of the direct runoff and the base flow at the previous time interval. (Chapman, 1999). After Chapman (1999) reformulation, Eckhardt (2008) has

mentioned that Long waves in a hydrograph's frequency range are more likely to be associated with base flow, while high-frequency variability in stream flow is mainly caused by direct runoff.(Eckhardt, 2008). Then base flow can be possibly identified by low- pass filtering the hydrograph. Then he improved new algorithm for base flow calculation and imply that the Chapman (1999) filter is a special case of his current algorithm. In this study, the three base flow filters mention above are tested for the DHRUM model calibration process. All equations used at the time of calculations are as follow:

This study focused on the two-component of streamflow which are direct runoff and base flow. The main equation is :

$$y_k = f_k + b_k$$

where k is the time step number,
y is the total stream flow,
f is direct runoff
b is the base flow.

The equation commonly used for base flow during dry period or so called non-recharge period with the assumption that the outflow from the aquifer is linearly proportional to its storage is as fallows:

$$b_{k+1} = b_k e^{\frac{-t}{\tau}} = ab_k$$

where where {t} is the time step length
k is the characteristic time constant,
a is recession constant.

$$a = e^{\frac{-t}{\tau}}$$

Lyne and Hollick (1979) digital filter equation

$$b_k = ab_{k-1} + \frac{1+a}{2}(y_k - y_{k-1})$$

subject to bk $\leq$ yk, where a is the filter parameter,
k is the time step number. Most importantly, subject to fk geq0 or, in terms of the baseflow equaition becames as:

$$b_k = ab_{k-1} + \frac{1-a}{2}(y_k + y_{k-1})$$

Chapman and Maxwell filter

$$b_k = \frac{a}{2-a}b_{k-1} + \frac{1-a}{2-a}y_k$$

or

$$b_k = \frac{3a-1}{3-a}b_{k-1} + \frac{1-a}{3-a}(y_k - y_{k-1})$$

subject to bk $\leq$ yk, where a is the filter parameter, k is the time step number.

Eckhardt filter

$$b_k = \frac{(1 - BFI_{max})ab_{k-1} + (1 - a)BFI_{max}yk}{1 - aBFI_{max}}$$

subject to bk $\leq$ yk, where a is the filter parameter, k is the time step number, BFImax is the maximum value of the base flow index that can be modeled by the algorithm. (Eckhardt, 2005)

The parameter a can be determined by a recession analysis while BFImax is non-measurable. Based on the presented preliminary results from Eckhardt (2005) study on how to construct recursive digital filters for baseflow separation it is suggested to select BFImax is 80 for perennial streams with porous aquifers, BFImax is 50 for ephemeral streams with porous aquifers, and BFImax is 25 for perennial streams with hard rock aquifers. (Eckhardt, 2005). As mentioned before parameter a can be determined by a recession analysis, for this study the methodology described in the Manual on Low-flow Estimation and rediction which developed by World Meteorological Organization (WMO) is followed for calculation of parameter a and BFImax and it is explained in the following section.

Base-flow index Calculation

In this study in the World Meteorological Organization (WMO) Manuel followed for the calculation for base flow index and recession parameter a. In the Manuel there is process of 8 step of calculation. (Gustard et al., 2009). Those steps in brief are:

- step1 : To Divide the time series of daily flows, Q (m³/s), into non-overlapping blocks of five days
- step2 : Select the minima of each five-day period, Qm
- step3: Identify the turning points in this sequence of minima (Qm) by considering, in turn, each minimum and its neighbouring minima values. In each case, if 0.9 x central value less then equal to adjacent alues, then the central value becomes a turning point, Qt
- step4 :Join the turning points, Qt , by straight lines to obtain the base-flow hydrograph;
- step5: Assign a base-flow value to each day by linear interpolation between the turning points. The base flow is constrained to equal the observed hydrograph on any day if the base-flow hydro- graph exceeds the observed flow
- step6:Continue this procedure until the complete time series has been analysed;
- step7 : The volume of water (m³) beneath the sepa- ration line (Vbase) for the period of interest is simply determined as the sum of the daily base- flow values multiplied by the time span in seconds per day. The volume of water beneath the recorded hydrograph (Vtotal) is calculated in the same way;
- step8: Lastly, BFI is determined as: BFI = Vbase /Vtota Gustard, Demuth, and others (2009)

Those calculation steps are available in R package lfsat which is named as Calculates Low Flow Statistics for daily stream flow data package. (Koffler et al., 2016; Gustard et al., 2009).

For calculation of BFImax R lfstat package is used and BFImax value are calculated for each 671 catchments separately following the manual process and the max value of BFI is assigned as BFImax for Eckhardt filter.

Recession analysis

Recession analyses for calculation of parameter a is flowed by WMO manual where the recession curve is modelled by fitting an analytical expression to the outflow function Qt which is assumed to be first-order linear storage with no inflow. Then parameter a can be defined as the slope of the curve fitted to the data points of discharge at the one-time interval (Qt–1) and discharge one-time interval later (Qt). There are two main groups of classification to identify and parameterize the characteristic recession behaviour of a catchment. One of them is a constructing structure of master recession curve(MRC), the other class is performing separate calculation of parameter also known as individual recession segments (IRS). For both cases, the recession segment is selected from the continuous record. However, the MRC approach attempts to solve the problem of segment fluctuations by constructing a mean recession curve. In this study, the MRC method is used for recession analyses. (Gustard et al., 2009)

In this study for all 671 catchments, a fixed threshold level of Q70 is selected. Despite the length of the recession period can be a constant or a varying number of time steps, 5 days of the segment is selected as the minimum number of days to be marked as a recession period. As it is suggested that 5 days of long duration to be a minimum duration recession period, the catchment that doesn't have at least 5 days of recession periods are eliminated from the calculation. The figure below is an example of recession analyses processes for the calculation of parameter a to be used in the base flow filter. The outputs are results from daily streamflow data of catchment with id 1030500 and named Mattawamkeag River near Mattawamkeag, Maine. The data period is approximately 5 years of observation data. The first figure 2.5shows theIdentification of recession periods from a continuous streamflow record data for 1,5 the hydrological year 1990/1991

The figure 2.6 shows the result of recession analyses of Parameter a and recession duration bar plots.

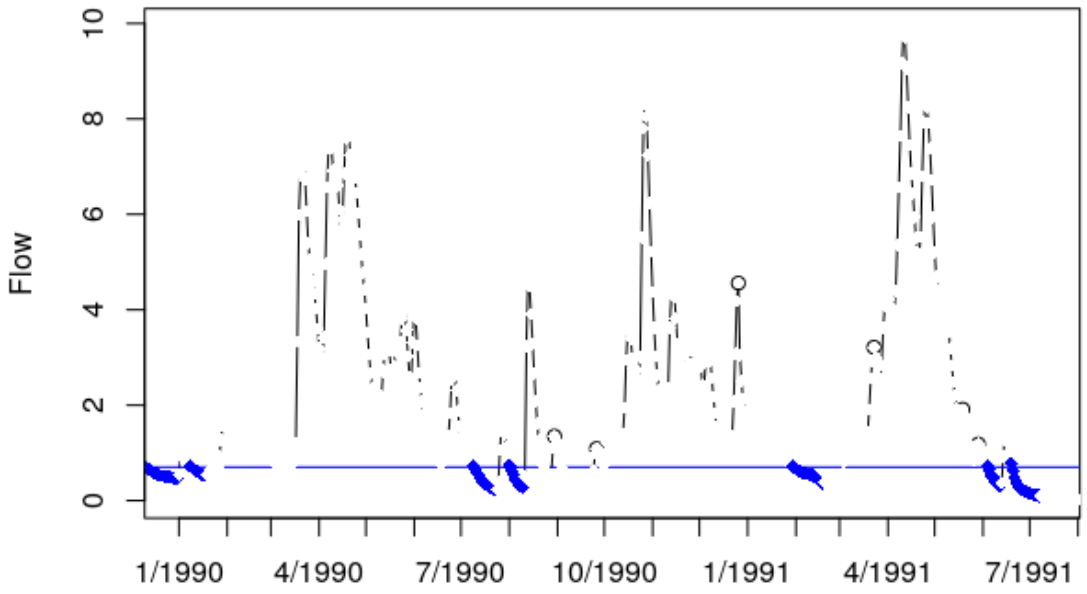

Figure 2.5: Recession periods from a continuous stream flow record

Following after proper a parameter calculation test on Mattawamkeag River near Mattawamkeag, the formula carried out for all the catchments and forcing. The figure 2.7below shows distribution of calculated recession parameter with nldas forcing data.

As it is stated the hydrological properties of soil, geology, and other storage-related descriptors are all strongly correlated with base-flowindices.Eckhardt (2005) proved that BFI_{max} value is high for perennial streams with porous aquifers, and BFI_{max} is low perennial streams for with hard rock aquifers. Then field investigation of hydrological conditions became essential to implement the Eckhardt method. However, there are several studies that have been done for the calculation of BFImax without field investigation of hydrological condition. For example, Collischonn, Fan (2013) used forward a backward filter method which uses the recession constant to calculate BFImax in his study "Defining parameters for Eckhardt's digital base flow filter". The backward filter method that uses the recession constant to calculate BFImax is a backward iterative operation executed on daily streamflow. The equation is as follows:

$$b_{k-1} = \frac{b_k}{a}(b_k \leq y_k)$$

where b is base flow y is stream flow and k is time step.

The BFImax values are calculated by dividing the maximum total base flow by total streamflow. Collischonn, Fan (2013) methods also tested by Xie et al. (2020) for the evaluation of typical methods for baseflow separation. As it has been proven that BFImax can be calculated

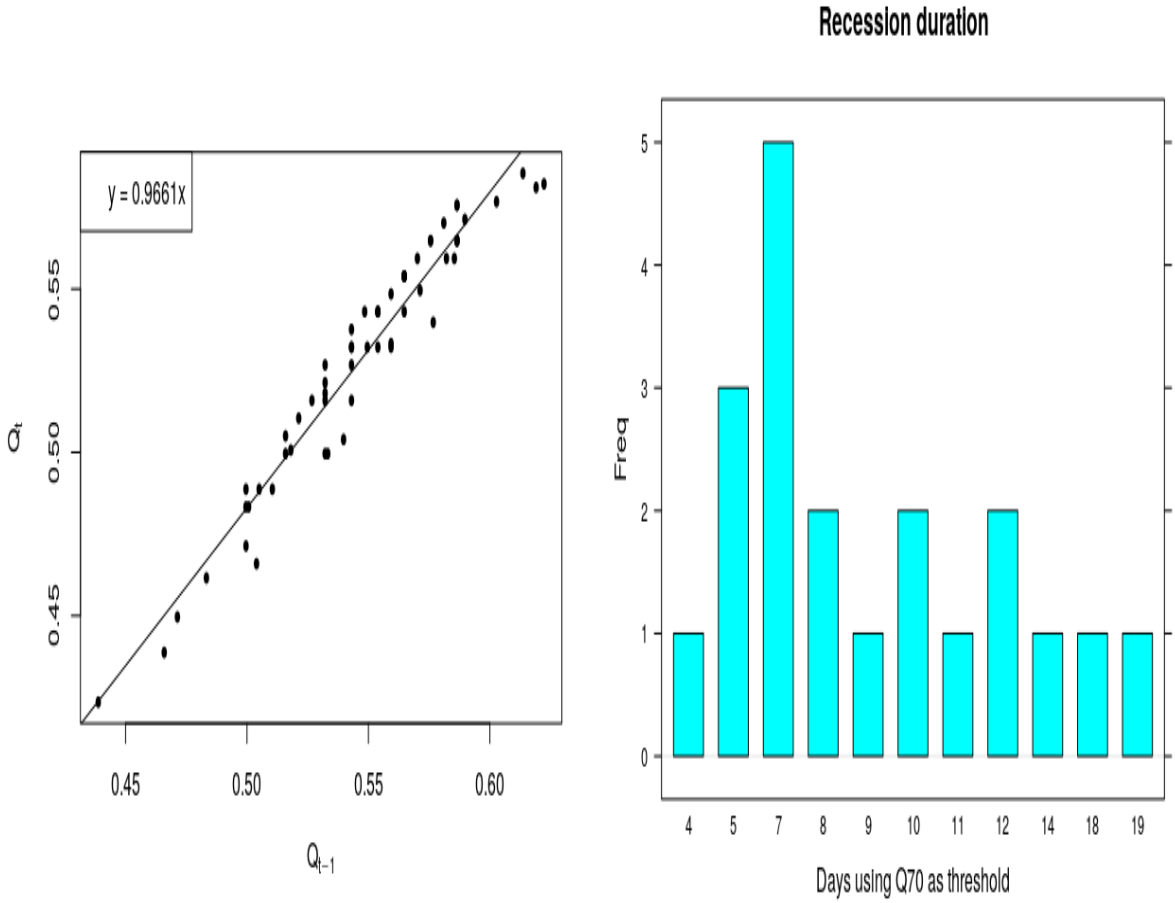

Figure 2.6: Recession calculation of parameter a, with recession duration

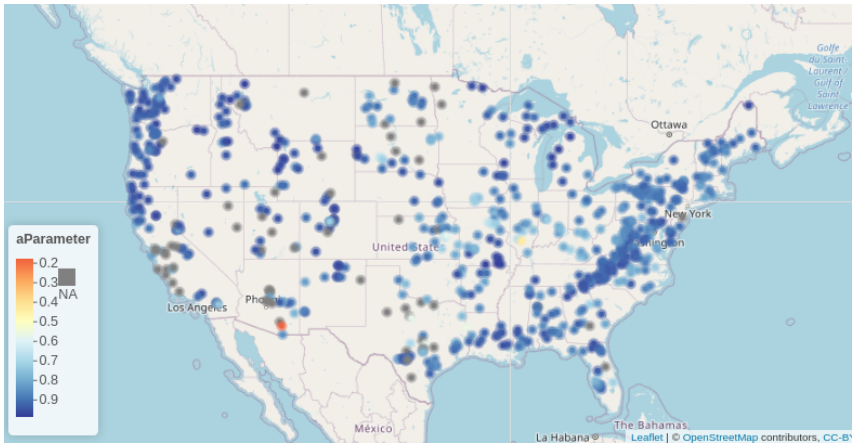

Figure 2.7: Calculated aParameter

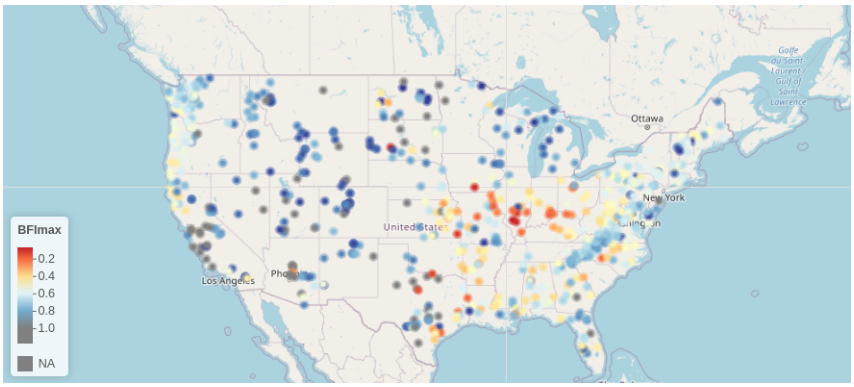

Figure 2.8: Calculated BFImax values

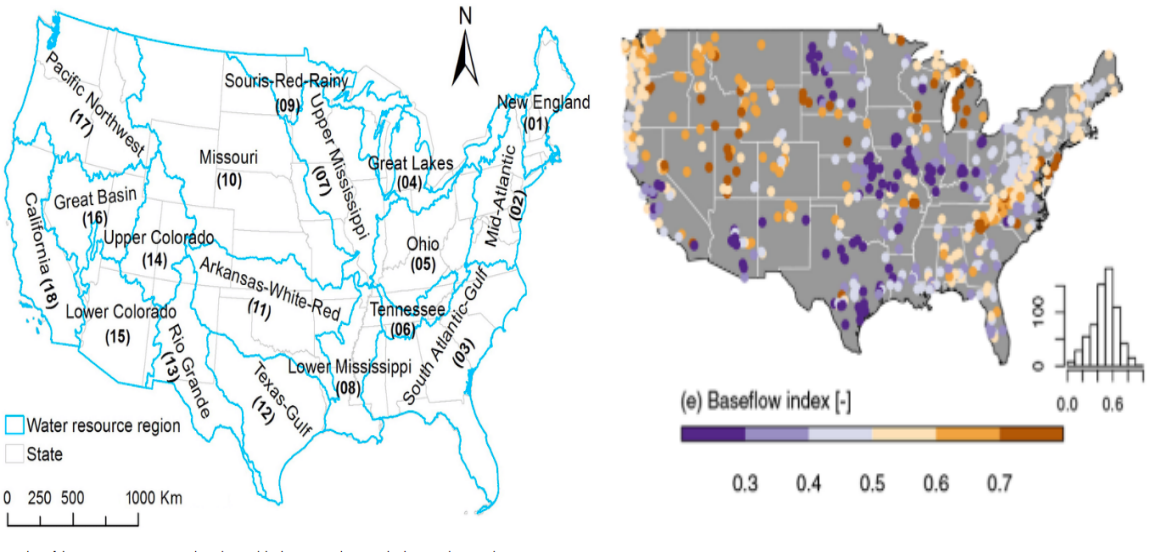

Figure 2.9: Figure left side is Location of the 18 water resource regions (WRRs) in the conterminous United States (CONUS), right fugure is analyzed baseflow Index by @Addor2017

by dividing the maximum total base flow to total streamflow without field investigation, in this study BFI max is calculated by division of base flow calculation from WMO Manuel steps to total streamflow. The results obtained from BFI max calculations are shown on the map 2.8.

As we can see from the map BFImax values are low in The Ohio, South Atlantic Gulf, Lower Mississipi regions. Those regions have low porosity fraction, low saturated hydraulic conductivity according to Addor et al. (2017). On the other hand, BFI max values are high in the Missouri, Upper Colorado regions. When we compare the BFImax values calculated in this study and the Baseflow Index over the CONUS map created by Addor et al. (2017) which is shown in the figure below the right side, we can see that there is a pleasing similarity between the two maps 2.9.

2.1.4 Optimization algorithm

In this study optimization algorithm of Global Optimization by Differential Evolution is used for the minimization of objective functions. Differential Evaluation is first introduced by Storn, Price (1997). There are three main steps that the differential evolution method consists of. The first step is to create a population with N individuals [x = (x1, x2, . . . , xm)] which is in the m-dimensional space, randomly distributed over the entire domain of the function in question and evaluation of the individuals of the so generated by finding f(x). The second step is to replace the current population with a better fit new population. The third step is repeating this replacement until satisfactory results are obtained. (Storn, Price, 1997). After Storm introduction, the algorithm has been explored extensively with successful performance as a global optimization algorithm. (Ardia et al., 2011). Later DE became a powerful tool for solving optimization problems. DE is also available in R with the package DEoptim. (Mullen et al., 2011).

As each optimization algorithm's main goal is to find the best value for model parameters based on numerical goodness-of-fit measures like minimizing or maximizing an objective function. In this study minimizing objective functions are measured. R package DEoptim is used for minimization. The value to be reached for minimization is selected as zero which is a VTR component of the DEoptim package. For that reason, 1- of each objective functions are selected as a fitness function of minimization. For example, NSE was an objective function 1 - NSE is selected as a fitness function for optimization with a minimal value of zero. Then strategy selected as 2 which is local to the best value. NP which is a number of population members is selected as 200 as it is suggested that to be at least 10 times of parameter vector which is in our case is 16 parameter. Furthermore, the crossover probability from the interval [0,1] is selected as 0.75. The figure 2.10 is an example of model output after optimization with 100 iterations for one of the catchments known as Fish River near Fort Kent, Maine.

2.1.5 Model calibration evaluation

For the model calibration evaluation, three evaluation indexes are adopted for grading the goodness-of-fit of the 671 CONUS catchments simulated flood hydrographs. These evaluation indexes are the mean and median value of the Nash-Sutcliffe coefficient, mean and median value of Kling-Gupta Efficiency and mean, the median value of Root Mean Square Error(RMSE). In order to measure the overall performance of model calibration, the absolute values of the evaluation indexes of the 671 catchments are averaged as follows:

Mean Nash-Sutcliffe coefficient

$$meanNSE = \frac{1}{M}\sum_{n=1}^{n=M}(1 - \frac{\sum_{n=1}^{M}(obs - sim)^2}{\sum_{n=1}^{M}(obs - mean(obs))^2})$$

Mean Kling-Gupta Efficiency(KGE)

$$meanKGE = \frac{1}{M}\sum_{n=1}^{n=M}(KGE)$$

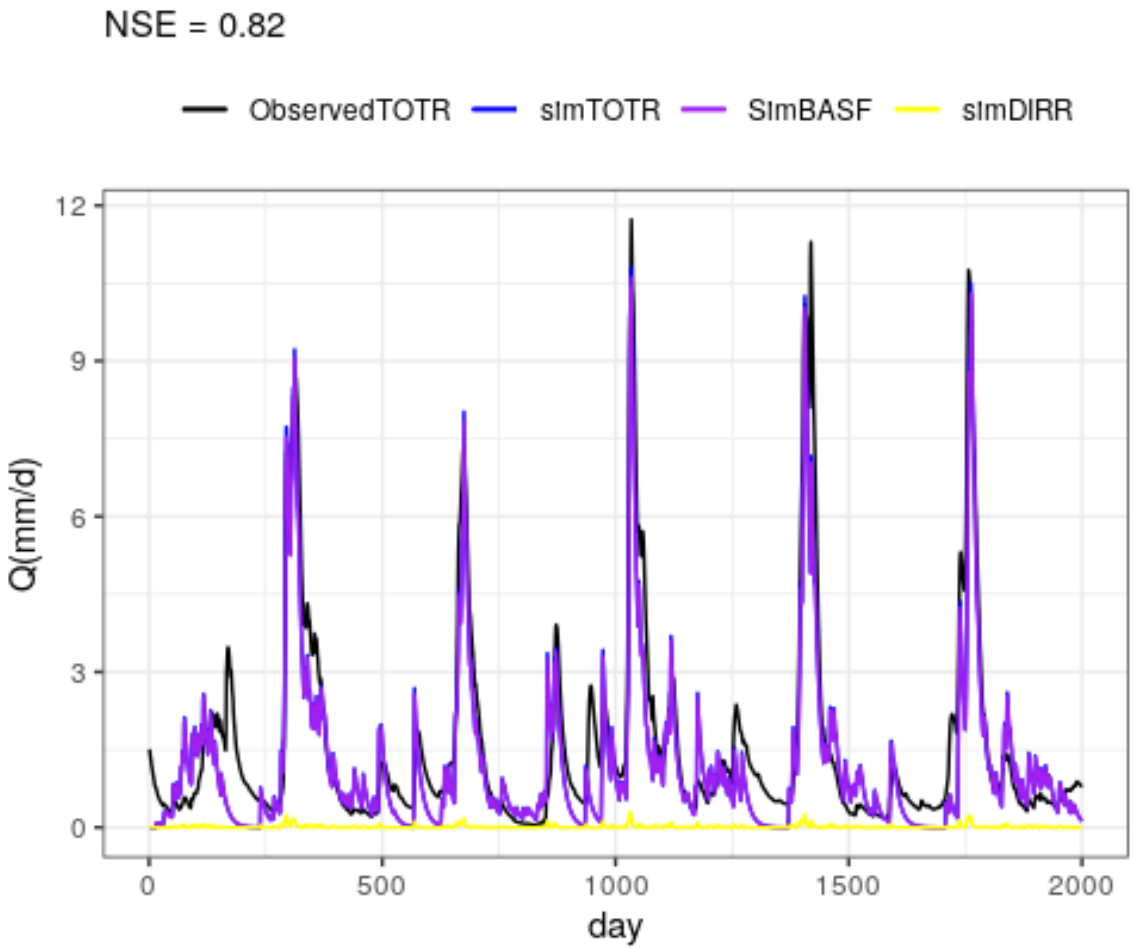

Figure 2.10: Fish River near Fort Kent, Maine optimized model outputs

Mean of Root Mean Square Error

$$meanRMSE = \frac{1}{M}\sum_{n=1}^{n=M}\sqrt{(\frac{1}{M}\sum_{n=1}^{M}(obs - mean(sim))^2}$$

RMSE is used for numerous studies for model performance evaluations as the minimum RMSE value represents the best combination of model parameters. (e.g (Adeyeri et al., 2020; Srivastava et al., 2017)) On the other hand, NSE compares the residual variance to the observed variance in terms of significance and NSE provides information on the models' performance on simulation of high flows .@Adeyeri2020 However Because of its periodicity, NSE may also return optimum values, giving a false impression of the model's capability. (Adeyeri et al., 2020). To avoid such a false impression of the models it is necessary to evaluate the model performance according to the connections between the variation coefficient and bias and ratios. In view of this KGE is an appropriate solution. (Gupta et al., 2009)

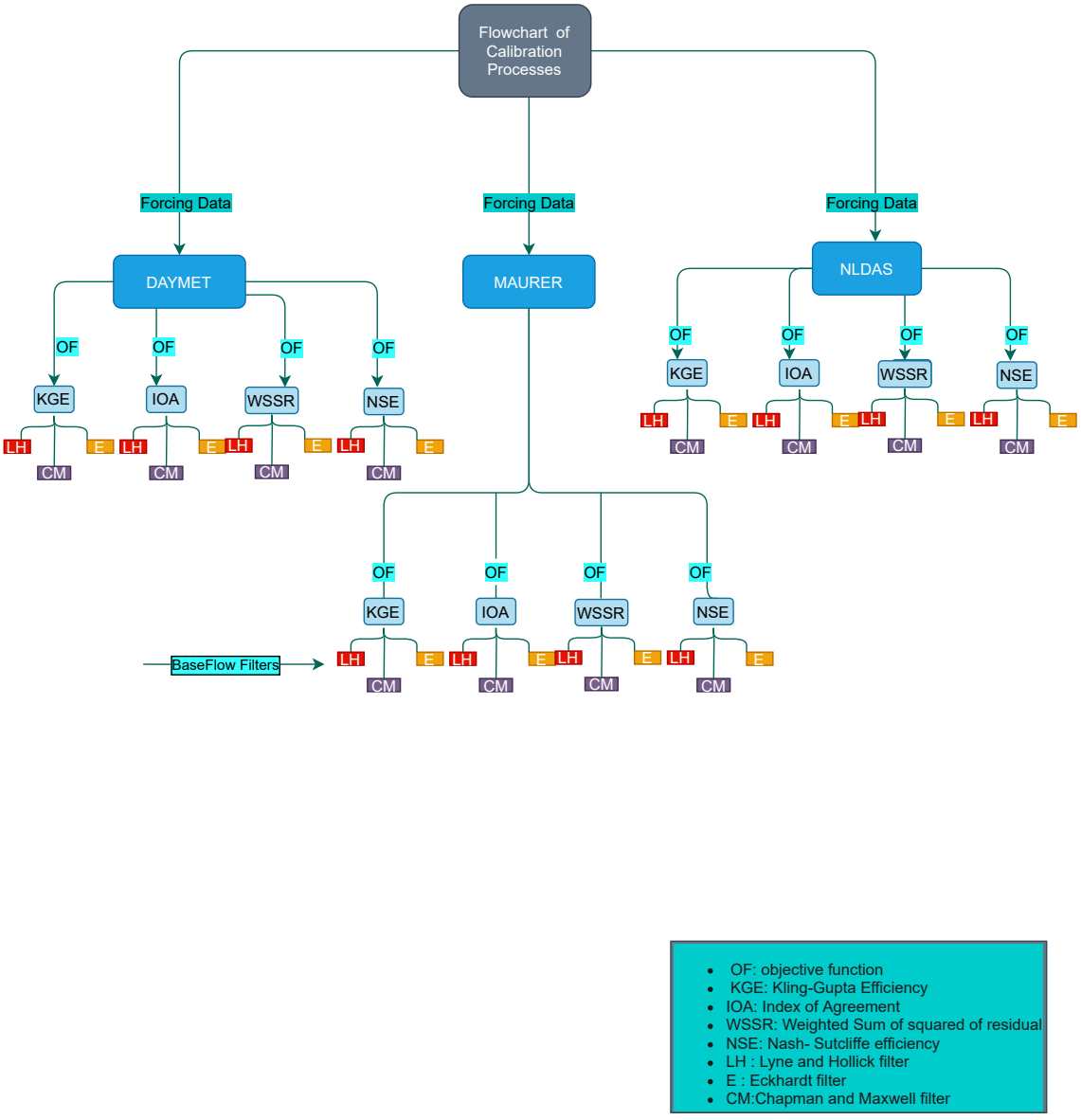

Figure 2.11: Flow Chart of the DHRUM Model calibration processes

CHAPTER 3

Results-and-Discussion

3.1 Results and Discussion

3.1.1 Summary of model total runoff generation after calibration with objective functions

The summary of the calibration with different objective functions computation is presented in the Table 3.1. The table represents the optimization of total runoff with four different objective functions which are Kling-Gupta Efficiency(kge), Index of Agreement(IOA), Nash-Sutcliffe Efficiency(nse) and Weighted sum of Square Roof of Residual(WSSR but named as "weighted" in all tables) and three different forcing data which are Nldas, Daymet and Maurer. During the calibration of the model, objective functions are used as explained in previous sections. In this section of calibration, simulated values are dHRUM total runoff outputs while observed values are measured streamflow data the results are the goodness of fit measures of total runoff generation. As the data set has 671 catchments and the some catchments have missing data which cause model failure with an extremely low value of efficiency such as nse of - 30, -25, the 10 per cent of those catchments are eliminated for mean and median values calculations. In addition to the summary table, the box plots and scatter plots of outputs are represented in figure 3.1.The box plot in figure 3.1 shows that the OF of NSE wirh Maurer data set has a significant impact on model performance while comparing the median values of all catchments performance.

Table 3.1: Result table of model total runoff generation after calibration with objective functions

	forcing	OF	MeanKGE	MeanNSE	MeanRMSE	MedianKGE	MedianNSE	MedianRMSE
1	daymet	IOA	0.29	0.05	2.55	0.380	0.05	1.980
2	daymet	kge	*0.40*	-0.04	2.71	0.430	-0.01	2.135
3	daymet	nse	0.23	*0.25*	2.31	0.250	0.21	1.740
4	daymet	weighted	0.26	0.14	2.41	0.290	0.12	1.920
5	maurer	IOA	0.34	0.13	2.32	0.460	0.17	1.830
6	maurer	kge	*0.44*	0.04	2.83	0.500	0.10	1.955
7	maurer	nse	0.30	*0.30*	2.28	0.340	0.30	1.720
8	maurer	weighted	0.31	0.22	2.44	0.375	0.22	1.820
9	nldas	IOA	0.32	0.10	2.35	0.410	0.14	1.980
10	nldas	kge	*0.41*	-0.02	2.83	0.450	0.03	2.130
11	nldas	nse	0.26	*0.27*	2.28	0.300	0.26	1.800
12	nldas	weighted	0.28	0.17	2.28	0.325	0.16	1.860

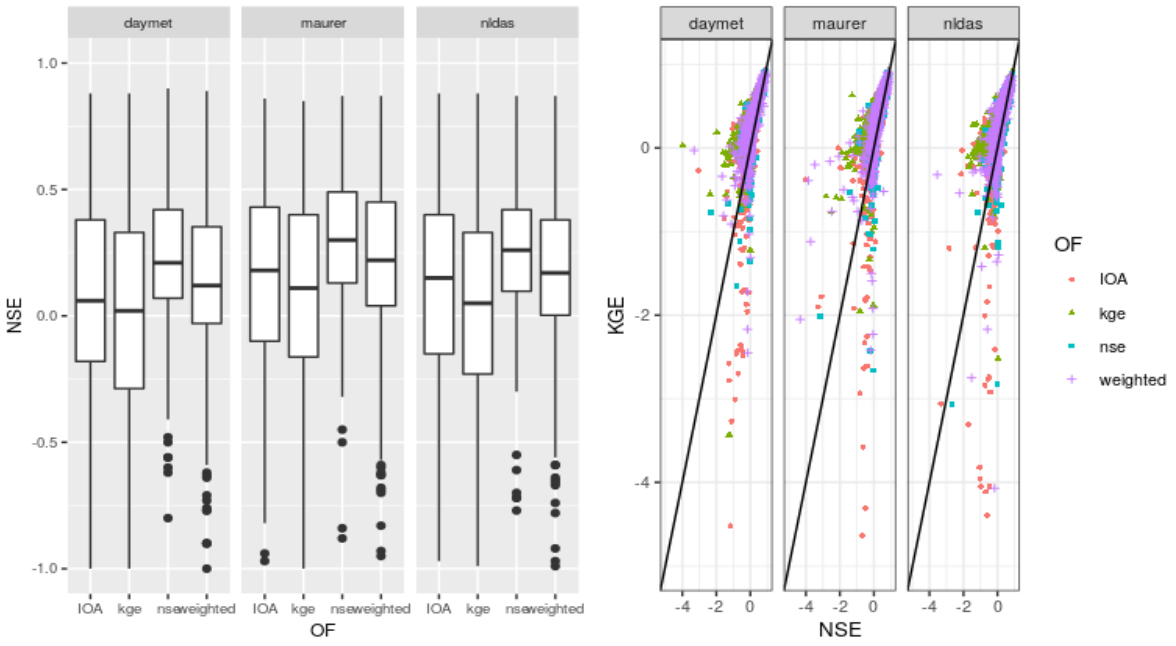

Figure 3.1: Scatter and box plots of the model calibration result for dHRUM with 4 objective functions and 3 forcings data

The result for the first episode show that the Daymet, Maurer and Nldas forcings data have mean KGE of best performance with the objective function of kge, with the value of 0.40, 0.44, 0.41 respectively. The results also show that for all forcing data and objective functions mean value of KGE are much higher than the mean use values of 671 catchments. On the other hand, the table shows that Daymet Maurer and Nldas forcing data have to mean nse of best performance with the objective function of nse with mean nse values of 0.25, 0.30, 0.27 respectively. Similarly, their mean RMSE best values are coming from calibration with the objective function of nse with RMSE values of 2.31, 2.28, 2.28 respectively. All in all, the table 3.1shows that Maurer forcing data has better performance with comparing to Nldas and Daymet data set and also Maurer forcing results in highest mean nse and lowest mean RMSE value which are 0.30 and 2.28 commonly.

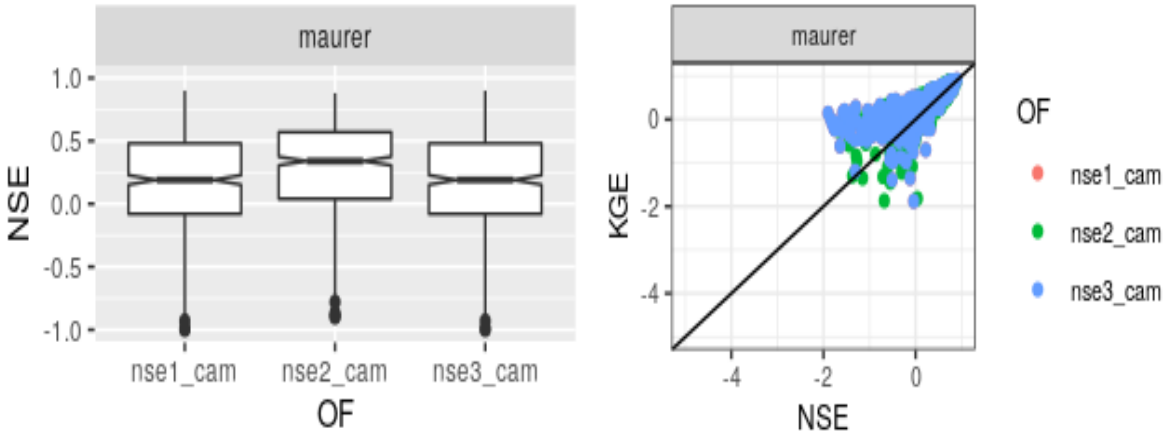

Figure 3.2: Scatter and box plots of the result of Calibration with objective Functions for three forcing data

After observing the best performance of Maurer data set with an objective function of nse in the first section of model calibration, the model performance of base flow simulation is generated. As base flow cannot be measured, it has to be calculated from different base flow calculation approaches as mentioned in the previous section. In this part, the observed values of base flow for model performance evaluation of baseflow are calculated from Lyne and Hollick, Chapman and Maxwell, and Eckhardt filters. In short, in this section the fitness function of model calibration is "1-nse" with the observed and simulated value of total runoff, however, performance evaluations are observed and simulated values of base flow. The table 3.2represents the model base flow calculation efficiency, with calibration of total runoff. Different from the first part here the model performance according to different base flow filter are generated. In the table 3.2. In the table nse_Chapman means the model calibrated with objective function of nse and observed values of base flow is generated from the Chapman filter and the model performance generated accordingly. Similarly for the other two scenarios which are Eckhardt and Lyne and Hollick(LH). In addition to the summary table 3.2, the box plots and scatter plots of outputs are represented in figure 3.2

Table 3.2: Result table model base flow generation after calibration with objective functions

	forcing	OF	MeanKGE	MeanNSE	MeanRMSE	MedianKGE	MedianNSE	MedianRMSE
1	maurer	nse_hapman	0.20	0.05	0.83	0.235	0.155	0.65
2	maurer	nse_Eckhardt	*0.28*	*0.26*	*0.96*	0.390	0.325	0.70
3	maurer	nse_LH	0.20	0.05	0.83	0.235	0.155	0.65

The result of the table shows that the dHRUM model generates better performance, when the observed values of baseflow are calculated with Eckhardt filter with mean KGE, mean NSE and mean RMSE with values of 0.28, 0.26, 0.96 respectively. In addition, the box plot in figure 3.2 shows that the Eckhardt filter has a significant impact on model performance with median values of all catchments performance.

3.1.2 Summary of model total runoff generation after calibration with base flow filters

The summary of the model optimization with different base flow filters computations is presented in the Table 3.3 The table represents the optimization of base flow with three different base flow filter functions which are Lyne and Hollick, Chapman and Maxwell, and Eckhardt filters and three different forcing data which are Nldas, Daymet and Maurer. During the calibration of the model, the objective functions of nse used as explained in previous sections. The model parameters are calibrated with the base flow generations. The simulated values are dHRUM base flow outputs while observed values are drived base flow from the filters and those values are used for fitness function of optimization. After model parameter calibration with the base flow, the modelled total runoff outputs are generated for the goodness of fit measures of total runoff efficiency.
Same procedure is applied the catchments that have missing data which cause model failure with an extremely low value of efficiency such as nse of - 30, -25, the 10 per cent of those catchments are eliminated for mean and median values calculations. In addition to the summary table, the box plots and scatter plots of outputs are represented in the figure 3.3.

Table 3.3: Result table of model total runoff generation after calibration with base flow filters

	forcing	OF	MeanKGE	MeanNSE	MeanRMSE	MedianKGE	MedianNSE	MedianRMSE
1	daymet	chapman	0.15	0.03	2.65	0.190	0.11	2.27
2	daymet	Eckhardt	*0.22*	*0.11*	2.55	0.250	0.15	2.09
3	daymet	LH	0.15	0.03	2.65	0.190	0.11	2.27
4	maurer	chapman	0.18	0.09	2.50	0.230	0.17	2.06
5	maurer	Eckhardt	*0.21*	*0.14*	2.45	0.260	0.20	2.03
6	maurer	LH	0.18	0.09	2.50	0.230	0.17	2.06
7	nldas	chapman	0.15	0.09	2.51	0.185	0.15	2.12
8	nldas	Eckhardt	*0.19*	*0.14*	2.46	0.230	0.18	2.05
9	nldas	LH	0.15	0.09	2.51	0.185	0.15	2.12

The result for the second episode shows that the Daymet, Maurer and nldas forcings have mean KGE of best performance with the objective of base flow filter function of Eckhardt filter, with the value of 0.22, 0.21, 0.19 respectively. The results also show that for all forcing data and base flow filters functions, the mean value of KGE are much higher than the mean nse values of 671 catchments when Chapman and Lyne and Hollick filters taken into consideration. However, for the case of nldas forcing with Eckhardt filter, the difference between mean kge and mean nse values are more related. In addition, the table shows that Daymet maurer and nldas forcing data have mean nse of best performance with fitness function of Eckhardt filter, with mean nse values of 0.11, 0.14 and 0.14 respectively. Furthermore, daymet forcing mean RMSE best values is observed from calibration of base flow with Eckhardt filter function with RMSE values of 2.55, while maurer and nldas forcing mean RMSE are 2.45 and 2.46 respectively. All in all, the table 3.3 shows that the Eckhardt filter has better performance on the calibration of total runoff and also Maurer forcing has better performance results with the highest mean nse and lowest mean

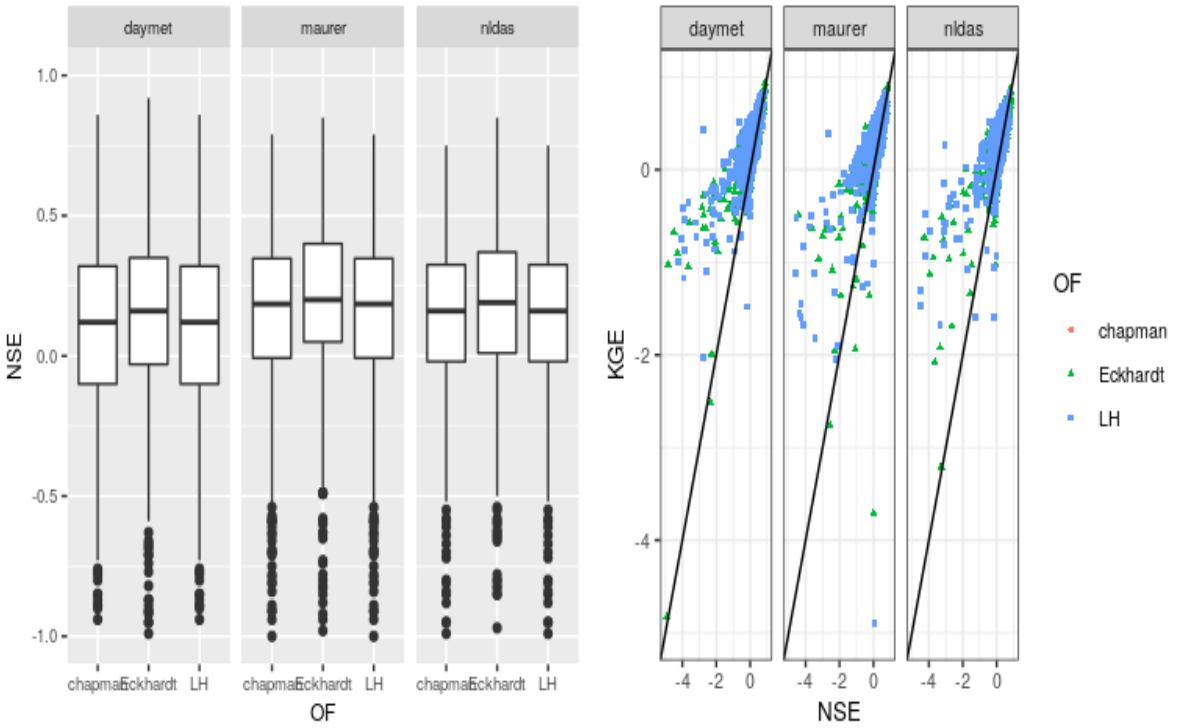

Figure 3.3: Scatter and box plots of the result of Total runoff Calibrated with Base flow through base flow filters

RMSE value which are 0.14 and 2.45 commonly.

3.1.3 Summary of model base flow generation after calibration with base flow filters

This part of model calibration follows the same procedure explained in episode two. However, this time after model parameter calibration with base flow, the modelled base flow outputs are generated for the goodness of fit measures of model base flow calculation efficiency in the fallowing table 3.4 and figure 3.4

Table 3.4: Result table of model base flow generation after calibration with base flow filters

	forcing	OF	meanNSE	medianNSE	meanKGE	meadianKGE	meanRMSE	medianRMSE
1	daymet	chapman	0.00	0.05	-0.10	-0.08	2.64	2.200
2	daymet	Eckhardt	*0.15*	*0.10*	0.03	0.02	2.48	2.050
3	daymet	LH	0.00	0.05	-0.10	-0.08	2.64	2.200
4	maurer	chapman	0.02	0.08	-0.09	-0.04	2.57	2.155
5	maurer	Eckhardt	*0.18*	* 0.14*	0.05	0.04	2.46	2.070
6	maurer	LH	0.02	0.08	-0.09	-0.04	2.57	2.155
7	nldas	chapman	0.02	0.07	-0.08	-0.05	2.57	2.190
8	nldas	Eckhardt	*0.15*	*0.13*	0.03	0.03	2.46	2.020
9	nldas	LH	0.02	0.07	-0.08	-0.05	2.57	2.190

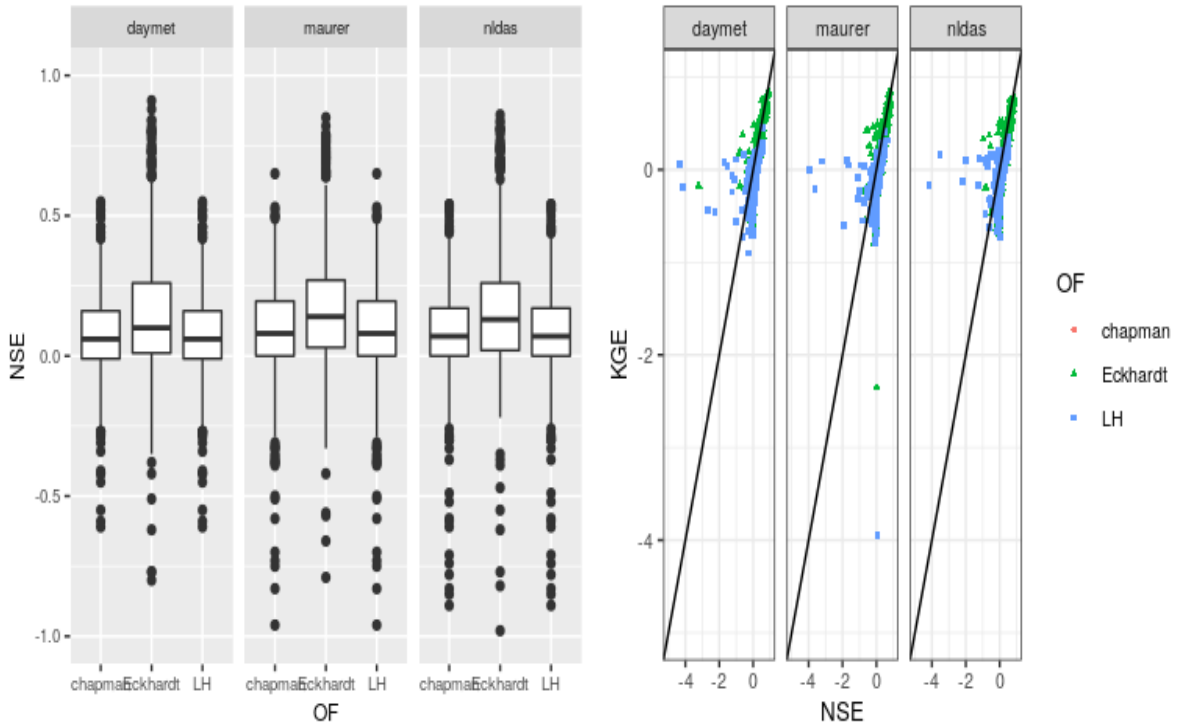

Figure 3.4: Scatter and box plots of the result of base flow generation after calibratio with base flow filters

3.1.4 summary-of-dHRUM model total-runoff-generation after calibration-with-weighted-functions functions

In this section, the dHRUM model is calibrated with linear combination of multi-objective functions. The objective functions explained in the section named selection of objective function and base flow filter are positive functions so, the parameters corresponding to the minimum value of the linear combination of each function are optimized by the DEOptim algorithm. In other words, this section represents the objective function called Weighted Sum of two different objective functions for total runoff and base flow calibration. Weights are calculated from the aridity index which is available in the CAMEL data set prepared by Addor et al. (2017). Aridity is calculated as the ratio of mean Potential Evapotranspiration which is estimated by N15 using Priestley–Taylor formulation calibrated for each catchment, to mean precipitation- (PET/P). According to Addor et al. (2017) study, the maximum value of the aridity index is 5.207 and the minimum value of the aridity index is 0.220. The calculation of W values are followed by linear interpolation between minimum and maximum aridity Index values in the range of weight from 0.3 to 0.9 . It has been shown that The main objective function is given by the formula below.

$$OF = W(OF1) + (1 - W)(OF2)$$

and OF1 is represent objective functions of total runoff OF2 is an objective function of base flow. The Figures 3.5 show the graph of Calculated Aridity values of each catchment byAddor et al.

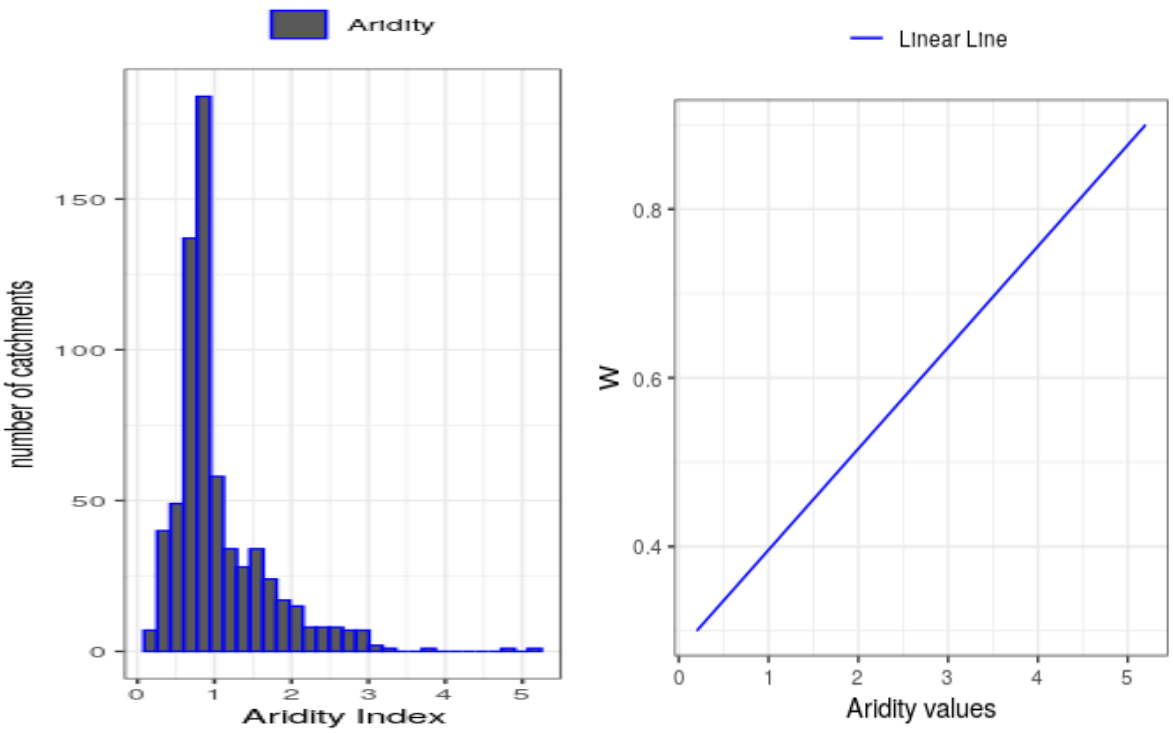

Figure 3.5: The avalible aridity Index values and linear interpolation values

(2017) and the linear interpolation values used in this study for calculation of W values.

then W1 weighted value for objective function of total runoff for each catchments calculated as presented formula below:

$$W = 0.3 + \frac{(0.9 - 0.3)}{(5.20 - 0.22)}(X_i - 0.2)$$

where Xi is aridity values of i th catchment and W is relative weighted values. In short and example in case of NSE as an objective function the formula becomes as follow

$$OF = W(1 - \frac{\sum_{n=1}^{M}(obsTOTR(i) - simTOTR(i))^2}{\sum_{n=1}^{M}(obsTOTR(i) - mean(obsTOTR(i)))^2})$$
$$+(1 - W)(1 - \frac{\sum_{n=1}^{M}(obsBASF(i) - simBASF(i))^2}{\sum_{n=1}^{M}(obsBASF(i) - mean(obsBASF(i)))^2})$$

Where i is the number of the observation, obsTOTR is the observed total runoff, simTOTR is the simulated total runoff, obsBASF is the observed base flow calculate from base flow filters simBASF simulated base flow. The summary of the model optimization with the Weighted Sum of two different objective functions for total runoff and base flow calibration computations are presented in the table below.

The table 3.5 represents the optimization of total runoff with three different base flow filter functions and three different forcing data and four different objective functions. After model parameter calibration, the modelled total runoff outputs are generated for the goodness of fit measures of total runoff efficiency. In addition to the summary table, the box plots and scatter plots of outputs are represented in the figures 3.6.

The result for the third scenario shows that the Daymet forcing performs best mean KGE value with objective function combination of kge and Eckhart filter with value of 0.39, while maurer forcing perform best mean KGE value with objective function combination of kge and Eckhart or Chapman filter with value of 0.42 and nldas forcing perform best mean KGE value with objective function combination of kge and Eckhart filter with a value of 0.40. It is clear that if evaluation criteria is mean kge model parameters better calibrated with a combination of KGE and Eckhardt filter and Maurer forcing. When mean NSE values are taken into consideration, the model parameters are calibrated with best performance of with a combination of nse and Eckhardt filter for all forcing data with the value of 0.23, 0.28, 0.26 for Daymet, Maurer, and nldas forcing respectively. Moreover, when the model performance is evaluated in terms of mean RMSE, Daymet, Maurer and nldas forcings show better performance with a linear combination of the objective function of nse and Eckhardt filter with mean RMSE values of 2.26, 2.27, 2.30 respectively. All in all, the table shows that the model parameter can be calibrated with the best performance with a linear combination of the objective function of nse and Eckhardt filter for three forcing data while Maurer forcing perform the best calibration of model parameters in terms of dHRUM total runoff generations.

Table 3.5: Result table of model total runoff generation after calibration with weighted functions

	forcing	OF	MeanKGE	MeanNSE	MeanRMSE	MedianKGE	MedianNSE	MedianRMSE
1	daymet	IOA_chapman	0.27	0.05	2.50	0.325	0.11	2.070
2	daymet	IOA_Eckhardt	0.28	0.09	2.43	0.340	0.14	2.020
3	daymet	IOA_LH	0.27	0.05	2.50	0.325	0.11	2.070
4	daymet	kge_chapman	0.37	0.02	2.53	0.390	0.07	2.175
5	daymet	kge_Eckhardt	*0.39*	0.05	2.63	0.390	0.08	2.095
6	daymet	kge_LH	0.37	0.02	2.53	0.390	0.07	2.175
7	daymet	nse_chapman	0.24	0.19	2.33	0.250	0.18	1.950
8	daymet	nse_Eckhardt	0.26	*0.23*	*2.26*	0.270	0.20	1.920
9	daymet	nse_LH	0.24	0.19	2.33	0.250	0.18	1.950
10	daymet	weighted_chapman	0.29	0.15	2.44	0.320	0.12	2.020
11	daymet	weighted_Eckhardt	0.28	0.16	2.43	0.300	0.13	2.090
12	daymet	weighted_LH	0.29	0.15	2.44	0.320	0.12	2.020
13	maurer	IOA_chapman	*0.32*	0.11	2.36	0.360	0.19	1.940
14	maurer	IOA_Eckhardt	*0.34*	0.15	2.34	0.380	0.23	1.940
15	maurer	IOA_LH	0.32	0.11	2.36	0.360	0.19	1.940
16	maurer	kge_chapman	*0.42*	0.11	2.40	0.450	0.19	1.940
17	maurer	kge_Eckhardt	*0.42*	0.14	2.36	0.450	0.20	1.900
18	maurer	kge_LH	0.40	-0.02	2.61	0.450	0.06	2.170
19	maurer	nse_chapman	0.29	0.25	2.27	0.320	0.25	1.900
20	maurer	nse_Eckhardt	0.32	*0.28*	*2.26*	0.350	0.27	1.800
21	maurer	nse_LH	0.27	0.21	2.36	0.340	0.24	1.880
22	maurer	weighted_chapman	0.35	0.23	2.29	0.410	0.23	1.910
23	maurer	weighted_Eckhardt	0.34	0.22	2.30	0.390	0.23	1.860
24	maurer	weighted_LH	0.35	0.23	2.29	0.410	0.23	1.910
25	nldas	IOA_chapman	0.29	0.12	2.33	0.340	0.18	1.960
26	nldas	IOA_Eckhardt	0.31	0.15	2.50	0.345	0.20	1.960
27	nldas	IOA_LH	0.24	0.01	2.58	0.340	0.06	2.190
28	nldas	kge_chapman	0.39	0.06	2.48	0.410	0.16	2.080
29	nldas	kge_Eckhardt	*0.40*	0.11	2.41	0.420	0.15	2.010
30	nldas	kge_LH	0.37	-0.04	2.64	0.410	0.03	2.190
31	nldas	nse_chapman	0.24	0.23	2.32	0.280	0.21	1.940
32	nldas	nse_Eckhardt	0.26	*0.26*	*2.30*	0.290	0.24	1.860
33	nldas	nse_LH	0.24	0.18	2.44	0.290	0.19	2.050
34	nldas	weighted_chapman	0.29	0.18	2.36	0.340	0.18	1.950
35	nldas	weighted_Eckhardt	0.29	0.18	2.36	0.330	0.18	2.025
36	nldas	weighted_LH	0.29	0.19	2.52	0.330	0.17	1.990

3.1.5 Summary of model base flow generation after calibration with weighted functions

The table 3.6 represents the optimization of base flow generation with three different base flow filter functions which are Lyne and Hollick, Chapman and Maxwell, and Eckhardt filters and three different forcing data which are nldas, daymet and maurer and four different objective functions. After model parameter calibration, the modelled total runoff outputs are generated for the goodness of fit measures of base flow efficiency. Same as previous sections the data set that have missing data which cause model failure with an extremely low value of efficiency such as nse of - 30, -25, the 10 persent of those catchments are eliminated for mean and median values calculations. In addition to the summary table, the box plots and scatter plots of outputs are represented in the figures 3.7.

The result for the third scenario shows that the model base flow generation outputs are not as good as model total runoff generation. The mean KGE, mean nse and mean RMSE values are

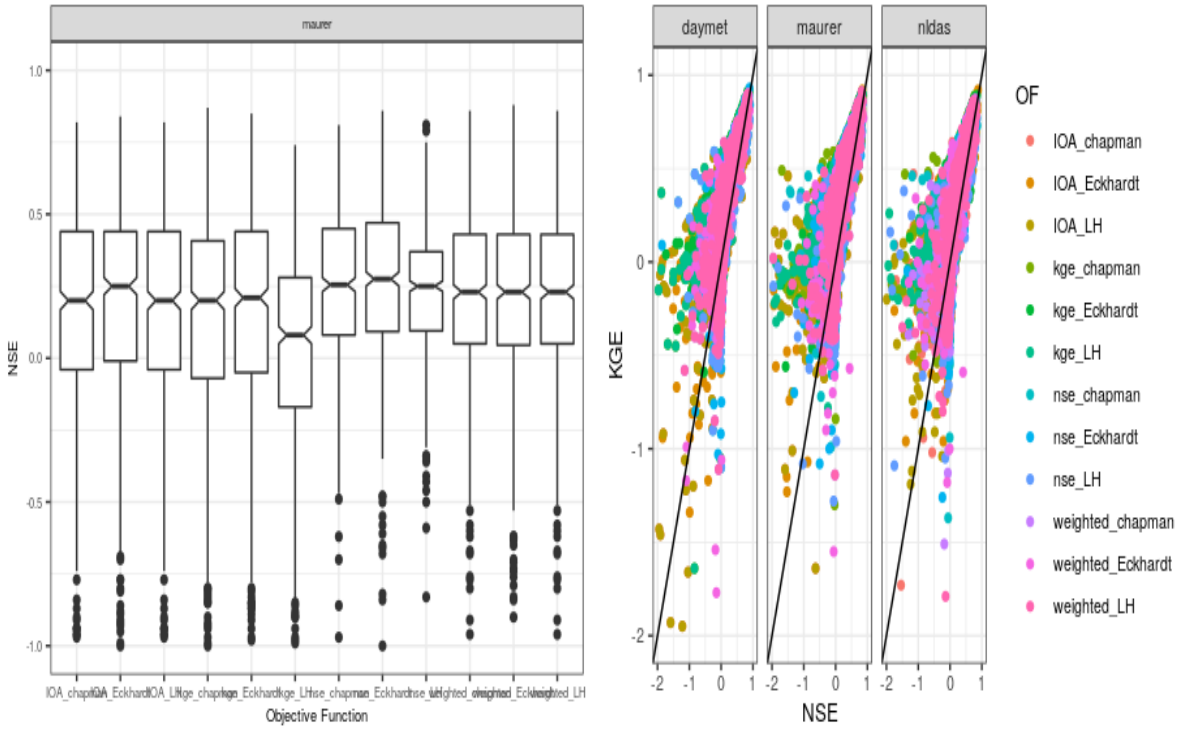

Figure 3.6: Boxplot and scatter plot of generated total runoff with calibration of Weighted functions

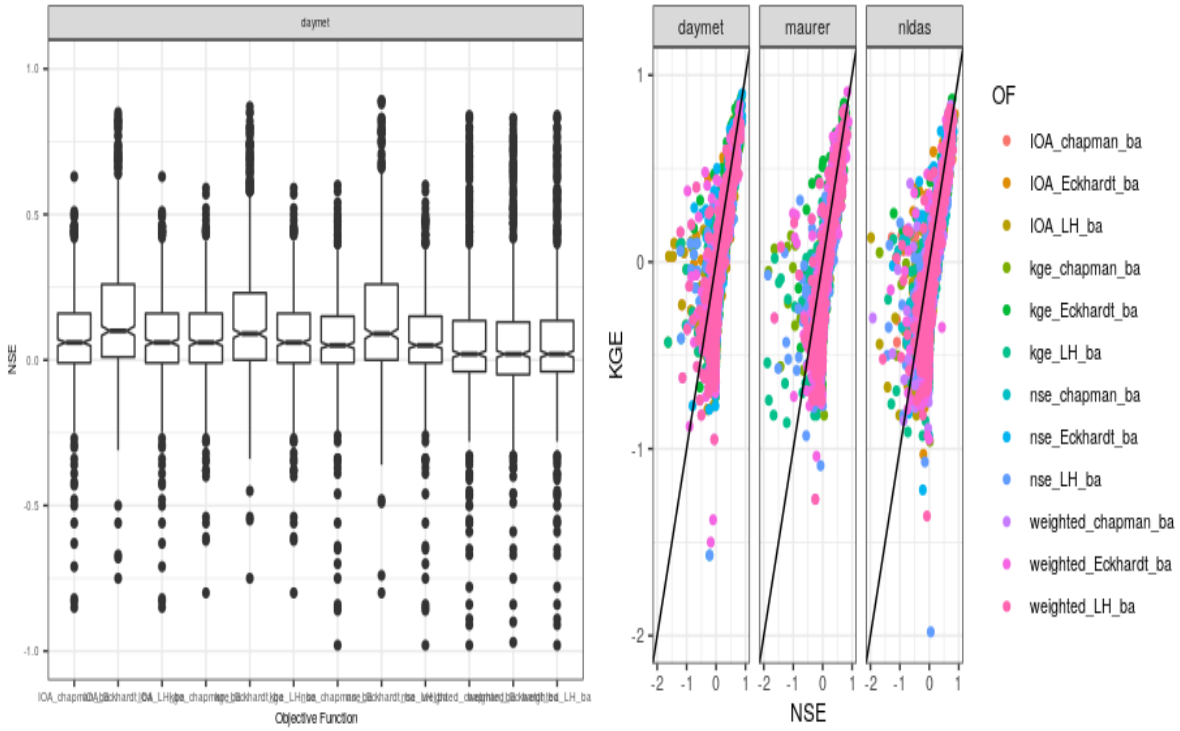

Figure 3.7: Boxplot and scatter plot of generated baseflow with calibration of Weighted functions

very poor with comparing total runoff outputs. However, it can be observed that three forcing data performed the best performance on base flow calibration with a linear combination of the objective function of nse and Eckhardt filter. The best performance values of mean KGE are 0.03, 0.03 and 0.04 which are pretty low. It is also shown that if evaluation criteria is mean nse model base flow generation has better calibration with the Eckhard filter. When mean NSE values are taken into consideration, the model parameters are calibrated with the best performance of with a combination of nse/IOA/kge and Eckhardt filter for all forcing data with value of 0.16, 0.16, 0.17 for Daymet, Maurer, and nldas forcing respectively. Moreover, when the model performance is evaluated in terms of mean RMSE, Daymet, maurer and nldas forcings show better performance with a linear combination of objective function f nse/IOA/kge and Eckhardt filter with mean RMSE values of 2.45, 2.41, 2.25 respectively. All in all, the table 3.6 shows that the model base flow generation can be calibrated with the best performance with a linear combination of the objective function of nse/IOA/kge and Eckhardt filter for three forcing data while Maurer forcing perform best calibration of the model parameters in terms of dHRUM base flow generation.

Table 3.6: Result table of model base flow generation after calibration with weighted functions

	forcing	OF	MeanKGE	MeanNSE	MeanRMSE	MedianKGE	MedianNSE	MedianRMSE
1	daymet	IOA_chapman	-0.09	0.06	2.57	-0.060	0.055	2.120
2	daymet	IOA_Eckhardt	0.02	0.16	2.44	0.020	0.100	2.000
3	daymet	IOA_LH	-0.09	0.06	2.57	-0.060	0.055	2.120
4	daymet	kge_chapman	-0.10	0.06	2.59	-0.070	0.060	2.205
5	daymet	kge_Eckhardt	0.02	0.15	2.60	-0.000	0.090	2.085
6	daymet	kge_LH	-0.10	0.06	2.59	-0.070	0.060	2.205
7	daymet	nse_chapmana	-0.10	0.06	2.58	-0.060	0.050	2.130
8	daymet	nse_Eckhardt	*0.0*3	*0.16*	2.41	0.010	0.090	2.025
9	daymet	nse_LH	-0.10	0.06	2.58	-0.060	0.050	2.130
10	daymet	weighted_chapman	-0.10	0.05	2.70	-0.140	0.020	2.180
11	daymet	weighted_Eckhardt	-0.09	0.07	2.66	-0.140	0.020	2.210
12	daymet	weighted_LH	-0.10	0.05	2.70	-0.140	0.020	2.180
13	maurer	kge_chapman	-0.08	0.07	2.58	-0.050	0.080	2.185
14	maurer	kge_Eckhardt	0.03	0.16	2.45	0.020	0.120	2.010
15	maurer	kge_LH	0.00	0.08	2.50	0.030	0.100	2.145
16	maurer	nse_LH	0.03	0.11	2.49	0.050	0.140	2.060
17	maurer	weighted_chapman	-0.12	0.05	2.65	-0.150	0.010	2.160
18	maurer	weighted_Eckhardt	-0.12	0.04	2.64	-0.165	0.010	2.200
19	maurer	weighted_LH	-0.12	0.05	2.65	-0.150	0.010	2.160
20	nldas	IOA_chapman	-0.08	0.07	2.48	-0.050	0.070	2.120
21	nldas	IOA_Eckhardt	0.03	0.16	2.58	0.030	0.120	1.980
22	nldas	IOA_LH	-0.00	0.08	2.52	0.030	0.090	2.200
23	nldas	kge_chapman	-0.09	0.07	2.59	-0.050	0.070	2.160
24	nldas	kge_Eckhardt	0.03	*0.16*	2.45	0.010	0.100	2.060
25	nldas	kge_LH_ba	-0.02	0.08	2.53	0.000	0.080	2.160
26	nldas	nse_chapman	-0.08	0.08	2.59	-0.050	0.075	2.165
27	nldas	nse_Eckhardt	0.04	0.17	2.47	0.030	0.120	2.030
28	nldas	nse_LH	0.00	0.09	2.56	0.020	0.110	2.200
29	nldas	weighted_chapman	-0.11	0.05	2.64	-0.160	0.010	2.120
30	nldas	weighted_Eckhardt	-0.11	0.06	2.63	-0.150	0.020	2.195
31	nldas	weighted_LH	-0.11	0.05	2.79	-0.170	0.010	2.200

The catchments considered in this study show a wide range of hydrological signatures and diverse climatic conditions. CAMEL data set has been analysed for many studies in order to quantitatively examine how the transection between topography, climate, land cover, soil, and geology affect the hydrological behaviour of the catchment. Xie et al. (2020); Jehn et al. (2019) analysed the impacts of catchment attributes on discharge characteristics in the whole CAMEL data set with catchment clustering 10 group. Jehn et al. (2019) has shown that, according to the weighted coefficient of determinations, climatic forcing mainly aridity and vegetation which is forest fraction are the most important for the discharge characteristics for many class of Camel data set. However, each class of CAMEL data has different attributes as the main driver impact on catchment discharge characteristics. The figure 3.8 shows the cluster of CAMEL data set analysed by Jehn et al. (2019). Those clusters and their defined attributes will be used to progress on a wide range of hydrological challenges related to catchments similarity and their impact on dHRUM model calibration performance variations.

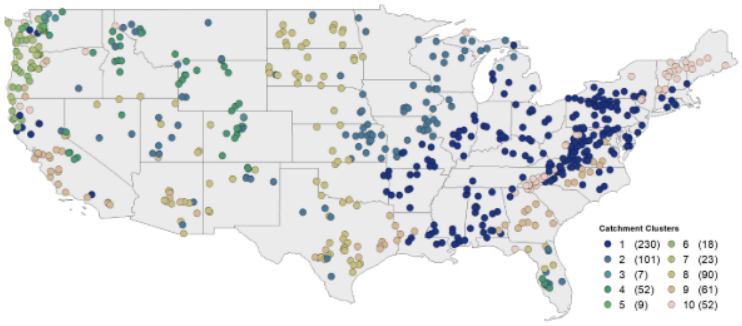

Figure 3.8: Locations of the clustered CAMELS catchments in the continental US (Jehn2019)

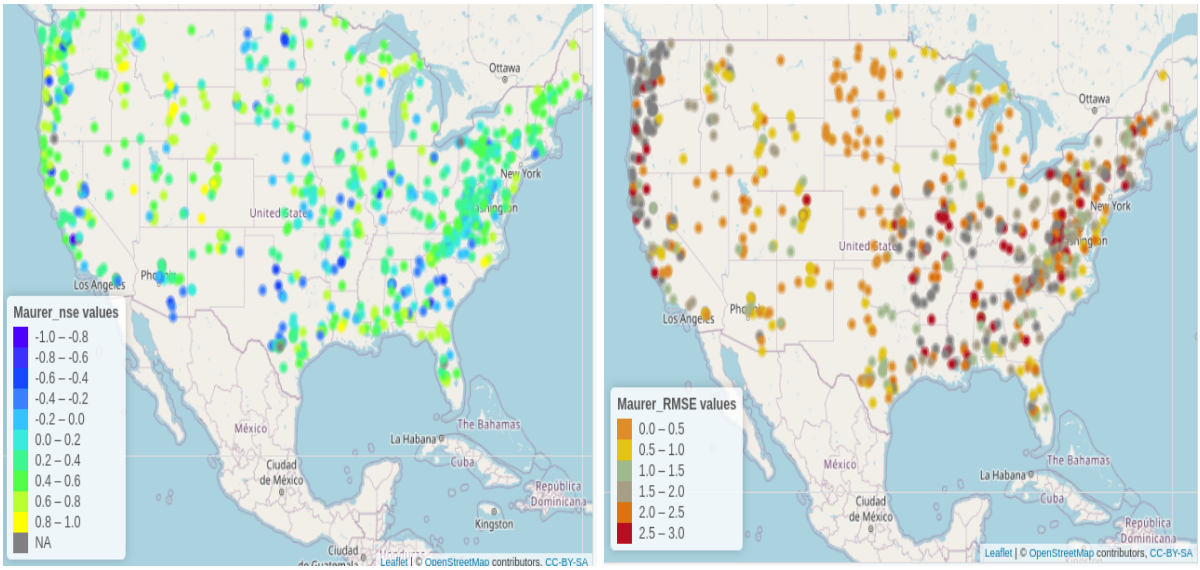

Figure 3.9: dHRUM model performance on total runoff generation with single objective function calibration evaluation according to evaluation criteria of NSE and RMSE in the conterminous United States (CONUS)

The figures 3.9 show that the model calibration with a single objective function. The performance of the model on a total run of generation has a wide range of distributions of efficiency according to NSE and RMSE measures. Although the applied calibration methods showed reasonable abilities to simulate total runoff with a satisfactory level of accuracy on most of the catchments caster, the number of catchments that showed very good calibration are relatively small. While considering Jehn et al. (2019) attributes classification of the catchment, it is observed that the model is well calibrated on the catchment cluster 6, 7 and 9 which are located on Marine West Coast Forests, Marine West Coast Forests and Southern states regions of CONUS. According to the Jehn et al. (2019) study those craters are which hydrological behaviour of the catchment has the clearest connection with aridity, a fraction of precipitation falling and aridity respectively. On the other hand, the distribution of nse and RMSE efficiency distribution shows that, the model is poorly calibrated on the catchment cluster 1, 2, 5 and 10 which are

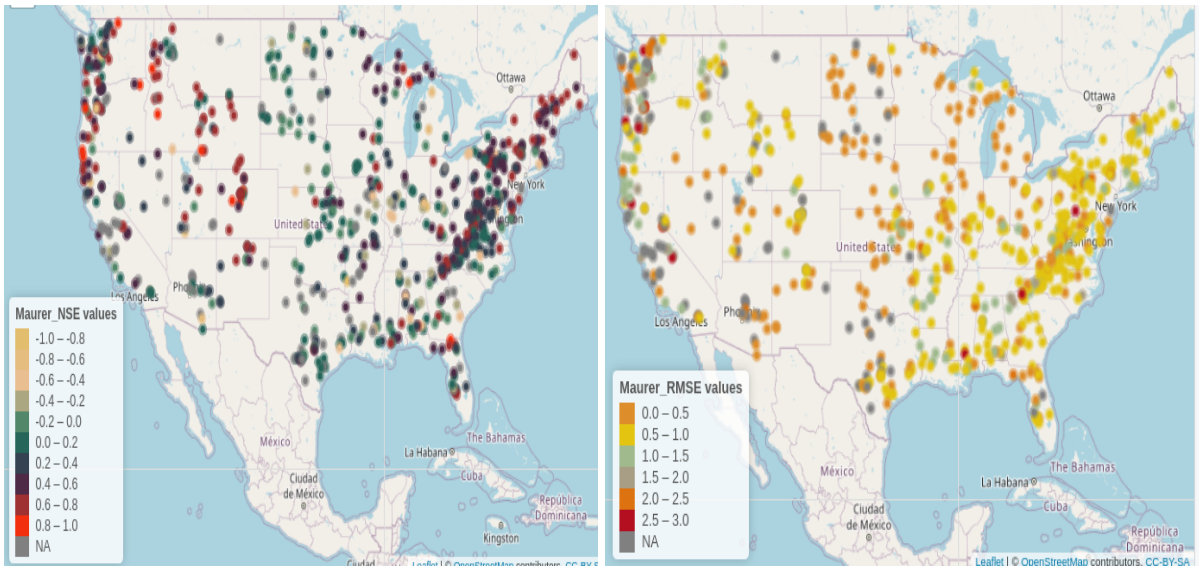

Figure 3.10: dHRUM model performance on base flow generation with single objective function calibration evalutaion according to evaluation criteria of NSE and RMSE in the conterminous United States (CONUS)

located on Southeastern and Central Plains, Central Plains, Northern Marine West Coast Forest, Appalachian Mountains. For those clusters hydrological behaviour of the catchment has the clearest connection with aridity, green vegetation maximum, forest fraction and mean elevation accordingly.

The figure 3.10 show that the model calibration with a single objective function. The performance of the model on base flow generation has a wide range of distributions of efficiency according to NSE and RMSE measures. Although the applied calibration methods showed reasonable abilities to simulate base flow with a satisfactory level of accuracy on most of the catchments caster, the number of catchments that showed very good calibration is relatively small.

However, the figure 3.7 shows that model calibration on base flow generation has a better interquartile range of efficiency comparing to total runoff generation which is represented in figure 3.6 The figure also represents that thenumber of catchments that has NA values while base flow generation is higher than the total runoff generation. That is the result of the elimination of catchment that doesn't have the appropriate condition for a parameter and BFImax calculations represented in the method section.

3.2 Conclusion

Different multi-objective and multi-base flow filter techniques have been evaluated in this study for the calibration of distributed Hydrological Response Unit Model hydrological model applied to the case of the 671 CONUS catchments with three different forcing data(Maurer, nldas and daymet forcing). The calibration process involved the use of four objective functions from goodness of fit measures (minimizingNSE, minimizingKGE, minimizingIOA, minimizing WSSR) and three base flow filters (Lyne and Hollick, Chapman and Maxwell, and Eckhardt filters). During the calibration evaluation of the model three scenarios are applied. These are model calibration with a single objective function to evaluate if it is sufficient to calibrate the dHRUM model only using a single objective function in terms of total runoff and base flow generations. The second scenario was model calibration with a single objective function of base flow filter to investigate if it is sufficient to calibrate the dHRUM model by using different base flow filters with observation of generated total run of and base flow measures. The last scenario was a linear combination of the objective function implemented in the first and second scenario to analyse the model performance improvement in terms of total runoff and base flow generations.

The calibration scenarios applied showed that they were capable of predicting runoff with a reasonable level of accuracy for most cases.

For the particular case of maurer forcing, its found that the objective function of nse and Eckhardt base flow filter methods performed best for both total run of and base flow generations. The lowest iterations and simulations were exhibited by the Lyne and Hollick filter for most of the cases. However in daymet forcing data cases Lyne and Hollick's filter showed the same calibration result which can be seen in the tables and plots. That problem accrued because of computational mistakes while writing the equation. After realizing the mistake the on daymet forcing scenarios, the formula for Lyne and Hollick filter is corrected and implemented to the rest of the calibration processes with maurer and nldas forcing data.

Based on these evaluations of three scenarios, it is observed that that the combination of multi-objective functions and multi-base flow filters techniques for optimal dHRUM model parameters calibration over the single objective function implementation not only improve the stability of the model parameters during calibration but also improve the optimization ability of the calibration algorithms towards the more accurate and robust representation of the river runoff in the basin. Despite there isn't considerable improvement in terms of mean values, the box plots showed that interquntile range of model performance is improved with calibration with weighted functions. It is also observed that due to the wide range of hydrological signatures and diverse climatic conditions of the catchments, the model calibration can be done according to catchment cluster's. Additionally, the evaluation of the model can be done accordingly.

Bibliography

Which objective function to calibrate rainfall–runoff models for low-flow index simulations? // Hydrological Sciences Journal. 2017. 62, 7. 1149–1166.

Addor Nans, Newman Andrew J., Mizukami Naoki, Clark Martyn P. The CAMELS data set: Catchment attributes and meteorology for large-sample studies // Hydrology and Earth System Sciences. 2017. 21, 10. 5293–5313.

Adeyeri O.E., Laux P., Arnault J., Lawin A.E., Kunstmann H. Conceptual hydrological model calibration using multi-objective optimization techniques over the transboundary Komadugu-Yobe basin, Lake Chad Area, West Africa // Journal of Hydrology: Regional Studies. 2020. 27. 100655.

Ardia David, Boudt Kris, Carl Peter, Mullen Katharine M., Peterson Brian G. Differential Evolution with DEoptim: An Application to Non-Convex Portfolio Optimization // The R Journal. 2011. 3, 1. 27–34.

Beven Keith. A manifesto for the equifinality thesis // Journal of Hydrology. 2006. 320, 1. 18–36.

Chapman Tom. A comparison of algorithms for stream flow recession and baseflow separation // Hydrological Processes. 1999. 13, 5. 701–714.

Collischonn Walter, Fan Fernando Mainardi. Defining parameters for Eckhardt's digital baseflow filter // Hydrological Processes. 2013. 27, 18. 2614–2622.

Deardorff James W. Efficient prediction of ground surface temperature and moisture, with inclusion of a layer of vegetation // Journal of Geophysical Research: Oceans. 1978. 83, C4. 1889–1903.

Duan Qingyun, Sorooshian Soroosh, Gupta Vijai. Effective and efficient global optimization for conceptual rainfall-runoff models // Water resources research. 1992. 28, 4. 1015–1031.

Eckhardt K. How to construct recursive digital filters for baseflow separation // Hydrological Processes. 2005. 19, 2. 507–515.

Eckhardt K. A comparison of baseflow indices, which were calculated with seven different baseflow separation methods // Journal of Hydrology. 2008. 352, 1-2. 168–173.

Ferket Bram V.A., Samain Bruno, Pauwels Valentijn R.N. Internal validation of conceptual rainfall-runoff models using baseflow separation // Journal of Hydrology. feb 2010. 381, 1-2. 158–173.

Fowler Keirnan, Peel Murray, Western Andrew, Zhang Lu. Improved Rainfall-Runoff Calibration for Drying Climate: Choice of Objective Function // Water Resources Research. 2018. 54, 5. 3392–3408.

Gupta Hoshin V., Kling Harald, Yilmaz Koray K., Martinez Guillermo F. Decomposition of the mean squared error and NSE performance criteria: Implications for improving hydrological modelling // Journal of Hydrology. 2009. 377, 1. 80–91.

Gustard Alan, Demuth Siegfried, others . Manual on low-flow estimation and prediction. 2009.

Hobeichi Sanaa, Abramowitz Gab, Evans Jason, Ukkola Anna. Derived Optimal Linear Combination Evapotranspiration (DOLCE): A global gridded synthesis et estimate // Hydrology and Earth System Sciences. 2018. 22, 2. 1317–1336.

Jehn Florian Ulrich, Bestian Konrad, Breuer Lutz, Kraft Philipp, Houska Tobias. Clustering CAMELS using hydrological signatures with high spatial predictability // Hydrology and Earth System Sciences Discussions. 2019. April. 1–21.

Jie Meng Xuan, Chen Hua, Xu Chong Yu, Zeng Qiang, Tao Xin E. A comparative study of different objective functions to improve the flood forecasting accuracy // Hydrology Research. 2016. 47, 4. 718–735.

Kim Jungwook, Kim Deokhwan, Joo Hongjun, Noh Huiseong, Lee Jongso, Kim Hung Soo. Case study: On objective functions for the peak flow calibration and for the representative parameter estimation of the basin // Water (Switzerland). 2018. 10, 5.

Koffler Daniel, Gauster Tobias, Laaha Gregor. lfstat: Calculation of Low Flow Statistics for Daily Stream Flow Data. 2016. R package version 0.9.4.

Li Hua, Nichols P. G.H., Han S., Foster K. J., Sivasithamparam K., Barbetti M. J. Differential Evolution – A Simple and Efficient Heuristic for Global Optimization over Continuous Spaces // Journal ofGlobal Optimization. 2009. 38, 3. 284–287.

Stochastic time-variable rainfall-runoff modelling. // . 1979. 1979. 89–93.

Maurer Edwin P, Wood Andrew W, Adam Jennifer C, Lettenmaier Dennis P, Nijssen Bart. A long-term hydrologically based dataset of land surface fluxes and states for the conterminous United States // Journal of climate. 2002. 15, 22. 3237–3251.

Mishra Surendra Kumar, Singh Vijay P. Soil conservation service curve number (SCS-CN) methodology. 42. 2013.

Mitsos Alexander, Chachuat Benoît, Barton Paul I. Global optimization of algorithms // AIChE Annual Meeting, Conference Proceedings. 2008.

Mullen Katharine, Ardia David, Gil David, Windover Donald, Cline James. DEoptim: An R Package for Global Optimization by Differential Evolution // Journal of Statistical Software. 2011. 40, 6. 1–26.

Nash J.E., Sutcliffe J.V. River flow forecasting through conceptual models part I — A discussion of principles // Journal of Hydrology. 1970. 10, 3. 282–290.

Newman A. J., Clark M. P., Sampson K., Wood A., Hay L. E., Bock A., Viger R. J., Blodgett D., Brekke L., Arnold J. R., Hopson T., Duan Q. Development of a large-sample watershed-scale hydrometeorological data set for the contiguous USA: Data set characteristics and assessment of regional variability in hydrologic model performance // Hydrology and Earth System Sciences. 2015. 19, 1. 209–223.

Piotrowski Adam P., Osuch Marzena, Napiorkowski Jarosław J. Joint Optimization of Conceptual Rainfall-Runoff Model Parameters and Weights Attributed to Meteorological Stations // Water Resources Management. 2019. 33, 13. 4509–4524.

Srivastava Ankur, Sahoo Bhabagrahi, Raghuwanshi Narendra Singh, Singh Rajendra. Evaluation of Variable-Infiltration Capacity Model and MODIS-Terra Satellite-Derived Grid-Scale Evapotranspiration Estimates in a River Basin with Tropical Monsoon-Type Climatology // Journal of Irrigation and Drainage Engineering. 2017. 143, 8. 04017028.

Staudinger M., Stahl K., Seibert J., Clark M. P., Tallaksen L. M. Comparison of hydrological model structures based on recession and low flow simulations // Hydrology and Earth System Sciences. 2011. 15, 11. 3447–3459.

Storn Rainer, Price Kenneth. Differential evolution–a simple and efficient heuristic for global optimization over continuous spaces // Journal of global optimization. 1997. 11, 4. 341–359.

Daymet: Daily Surface Weather Data on a 1-km Grid for North America, Version 2. // . ????

Willmott Cort J., Robeson Scott M., Matsuura Kenji. A refined index of model performance // International Journal of Climatology. 2012. 32, 13. 2088–2094.

Xia Youlong, Mitchell Kenneth, Ek Michael, Cosgrove Brian, Sheffield Justin, Luo Lifeng, Alonge Charles, Wei Helin, Meng Jesse, Livneh Ben, others . Continental-scale water and energy flux analysis and validation for North American Land Data Assimilation System project phase 2 (NLDAS-2): 2. Validation of model-simulated streamflow // Journal of Geophysical Research: Atmospheres. 2012. 117, D3.

Xie Jiaxin, Liu Xiaomang, Wang Kaiwen, Yang Tiantian, Liang Kang, Liu Changming. Evaluation of typical methods for baseflow separation in the contiguous United States // Journal of Hydrology. 2020. 583, August 2019. 124628.

Yapo Patrice Ogou, Gupta Hoshin Vijai, Sorooshian Soroosh. Multi-objective global optimization for hydrologic models // Journal of Hydrology. 1998. 204, 1-4. 83–97.

Yu Pao Shan, Yang Tao Chang. Fuzzy multi-objective function for rainfall-runoff model calibration // Journal of Hydrology. 2000. 238, 1-2. 1–14.

Zhang Lu, Potter Nick, Hickel Klaus, Zhang Yongqiang, Shao Quanxi. Water balance modeling over variable time scales based on the Budyko framework – Model development and testing // Journal of Hydrology. 2008. 360, 1. 117–131.

CHAPTER 4

appendix

4.1 Appendix

Base flow calculation according to three different baseflow filter

The figure 4.1 represent base flow calculation with three diffrenet base flow filters. Figure left side is correct representation of calculation on one of the catchments. However the figure on the right side shows the miscalculation of Line and Hollic filter that compiled in all scenarios of this study. The main reason of the difference is that the condition of fk >0 is not taken into consideration while calculations. The figure 4.2 represent Boxplot and scatter plot of generated base flow with calibration of Weighted functions. The figure 4.3 shows boxplot and scatter plot of model total runoff generations after calibration with combination of weighted functions. Distribution of model total runoff and base flow generation efficiency Maps from scenario with calibration of linear combination of objective functions are represented in figures 4.4 and 4.5

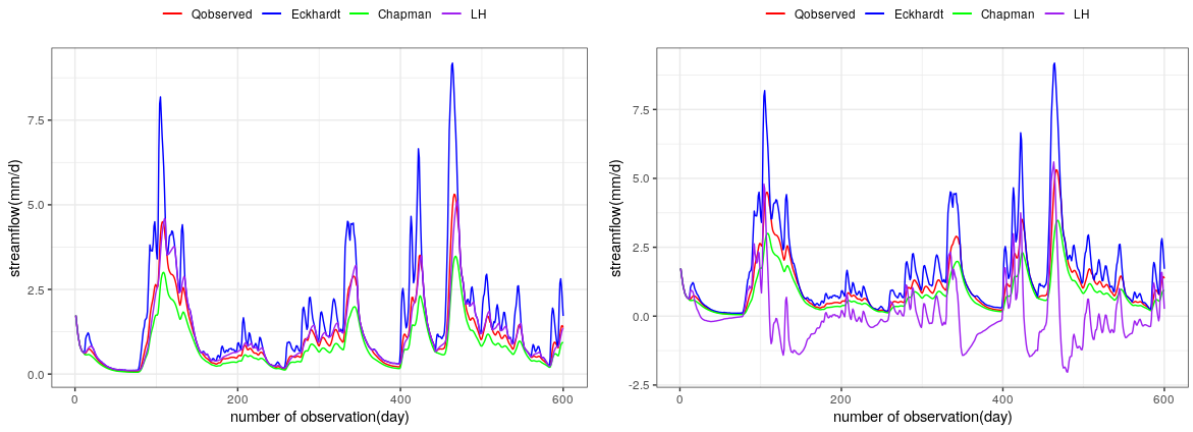

Figure 4.1: Calculated base flow with base flow filter

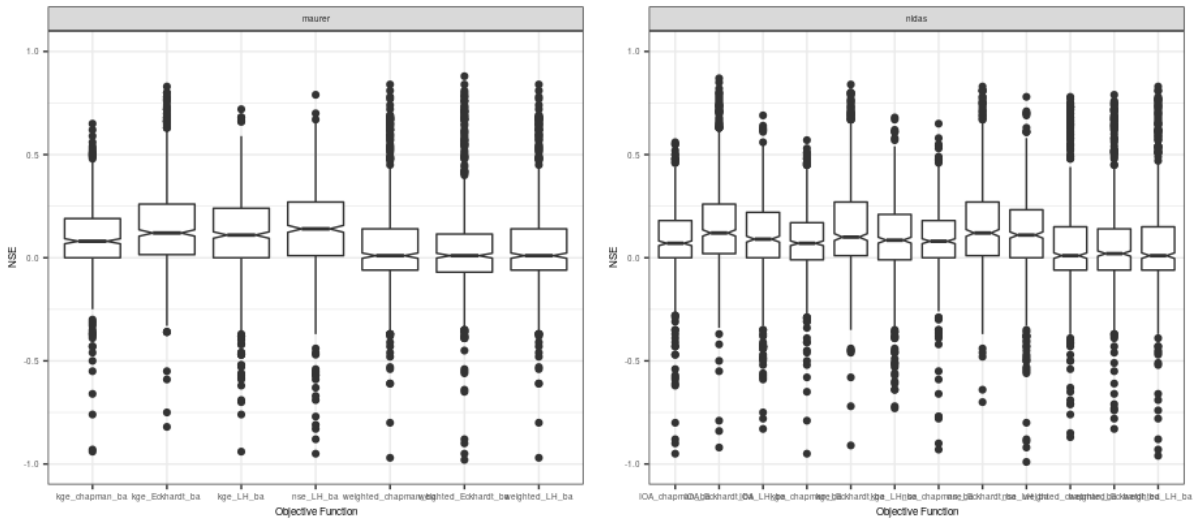

Figure 4.2: Boxplot and scatter plot of generated baseflow with calibration of Weighted functions

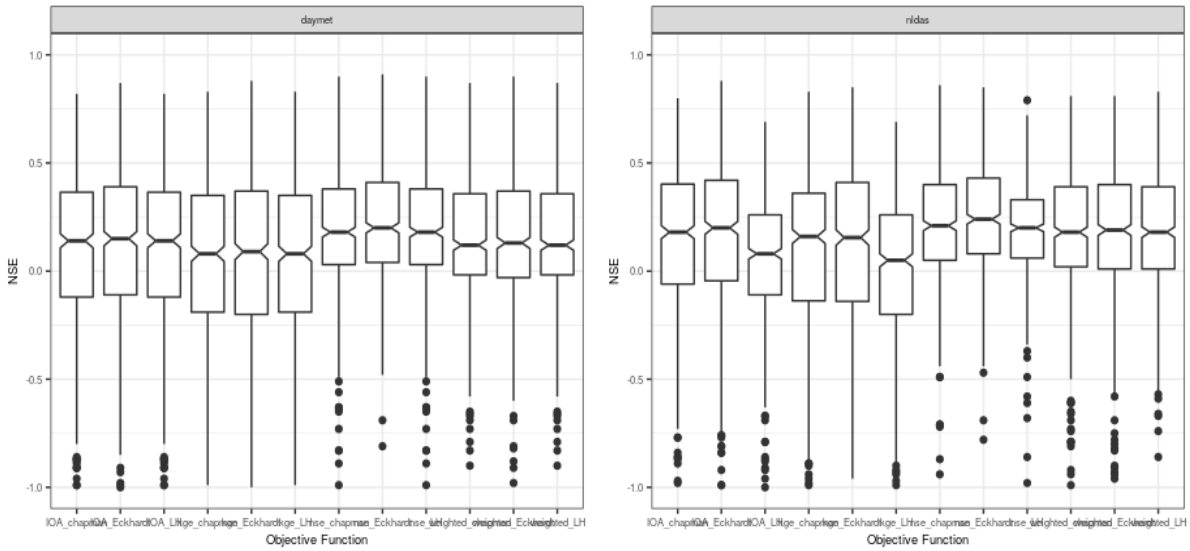

Figure 4.3: Boxplot and scatter plot of generated Total Runoff with calibration of Weighted functions

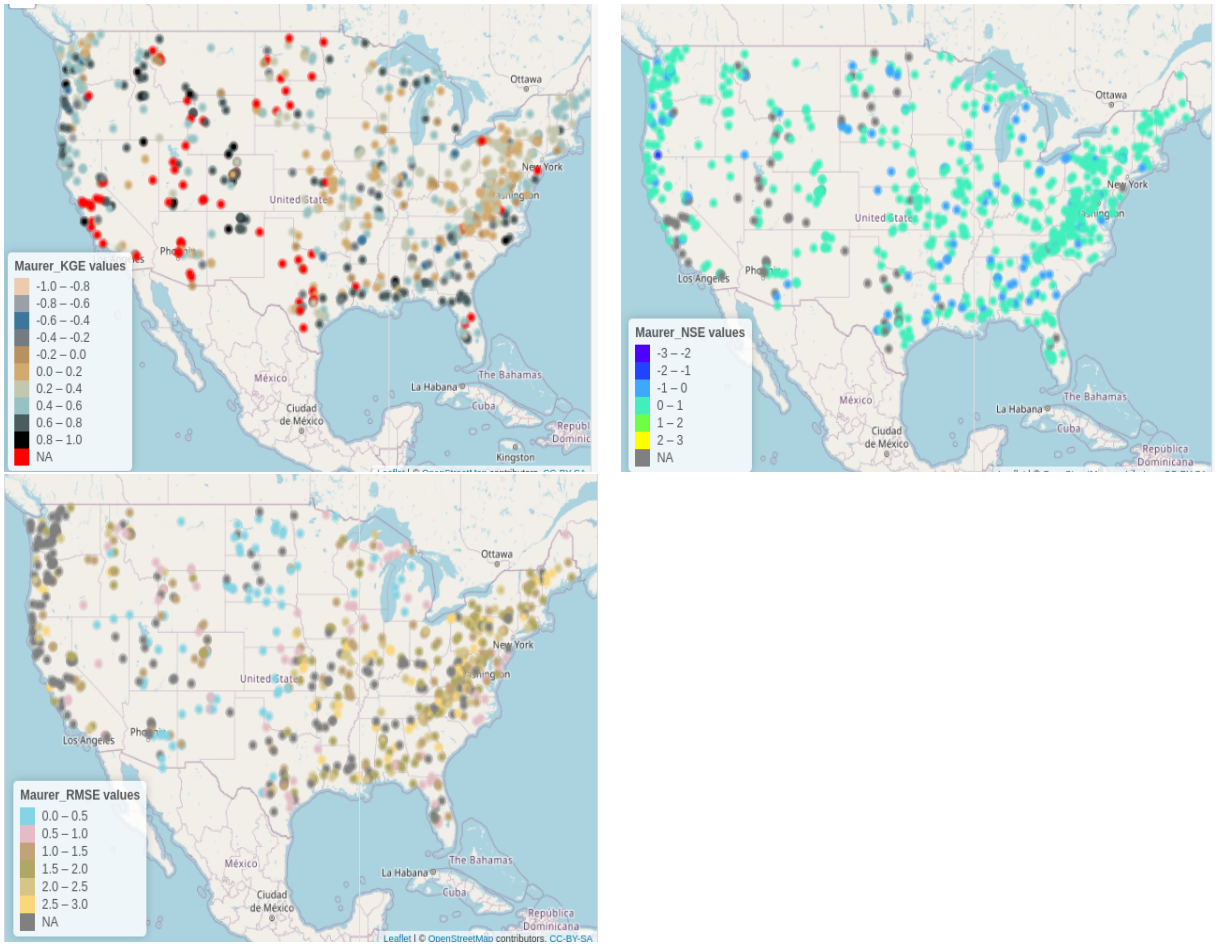

Figure 4.4: Distribution of model total runoff generation efficiency Map from scenario 3

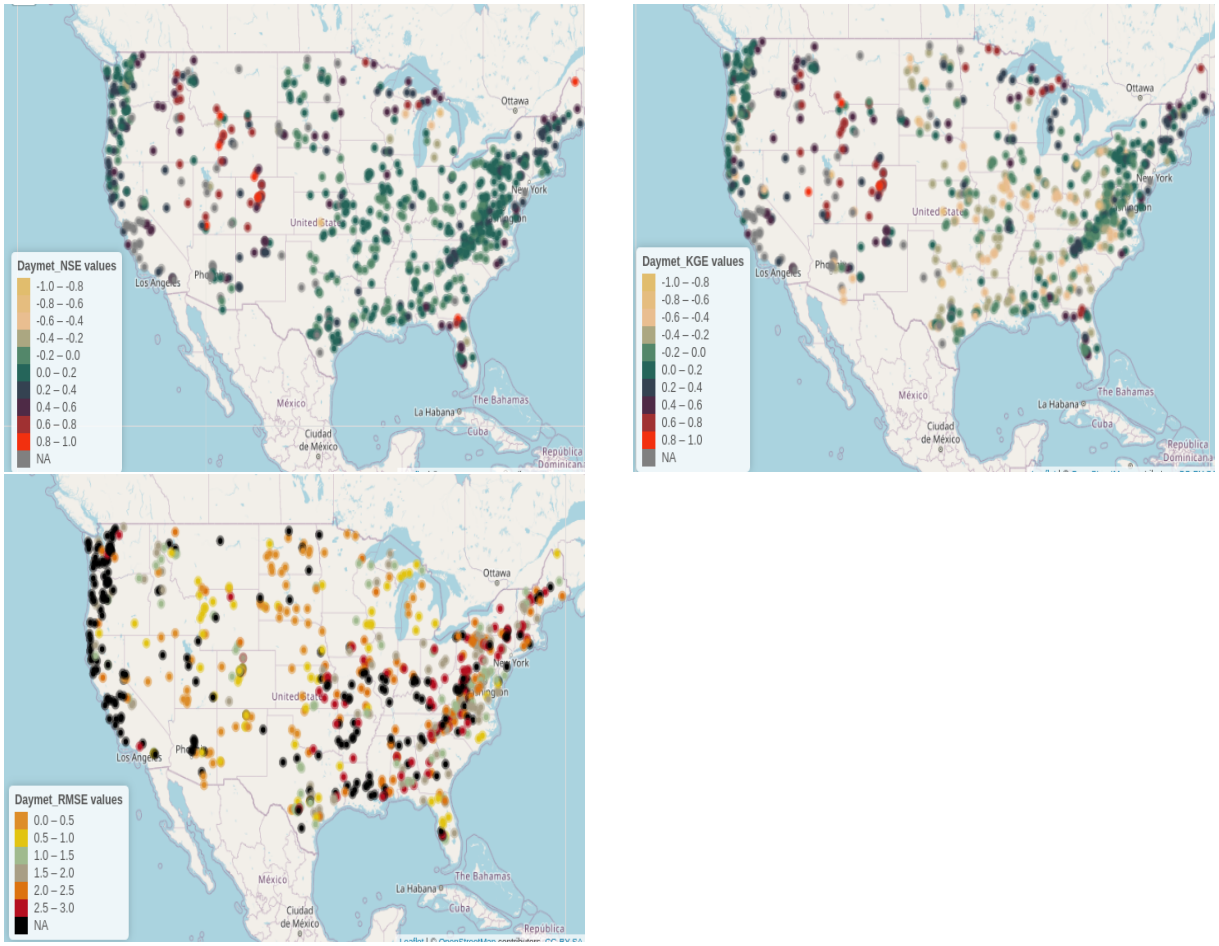

Figure 4.5: Distribution of model base flow generation efficiency Map from scenario 3